Aquatic Pollutants

REWA

Reduction and assessment of antimicrobial resistance and emerging pollutants in natural-based water treatment systems

D1.5 Final technical report (public)

Executive Summary

The document contains the final technical report on the reduction and assessment of antimicrobial resistance and emerging pollutants in natural-based waters (REWA) project. The main objective of the REWA project is the removal of contaminants of emerging concern (CECs) aiming for water reuse.

The project focused on the methods used for synthesizing and characterizing various materials, along with conducting pilot studies to assess their effectiveness in water treatment. The preparation and characterization of adsorbents such as iron-modified peat, tannin-based coagulants, biochar, and various nanocomposites were central to removing contaminants like antibiotics, metals, and emerging pollutants from water. Additionally, designs and methodologies for pilot-scale equipment aimed at removing pharmaceuticals from wastewater effluent were developed.

The case studies demonstrated the effectiveness of selected water treatment technologies for treating polluted surface waters, sewage effluents, and metal-rich effluent. In case study #1, several organoclays and photocatalyst such as modified bentonites, sepiolite and TiO_2/H_2O_2 were tested for CECs removal. For example, carbamazepine was removed through two different clay-based materials via adsorption and photocatalytic degradation. Mechanism for the photocatalytic degradation of carbamazepine (CBZ), showed pseudo-first-order kinetics at low concentrations and pseudo-zero-order at high concentrations. Also, the degradation of ofloxacin by combining UV/TiO_2, UV/H_2O_2, and $UV/TiO_2/H_2O_2$ and showed that combined photocatalysis yields higher pseudo-order. A pilot device for efficient photocatalytic degradation of such pollutants was developed, planned and built. Preliminary tests indicate efficient photodegradation of some pollutants in wastewater from the largest wastewater plant in Israel. Zinc removal from industrial wastewater effluent was examined using chelation modification of activated carbon. The quercetin-modified carbon exhibited enhanced zinc adsorption, particularly with granular forms, providing efficient and selective removal in water treatment applications. Additionally, a novel colorimetric method was developed for quantifying residual poly-DADMAC, a polymer commonly used as a modifier for clay-based coagulants in water treatment. The use of clay-based coagulants for the efficient removal of cyanobacteria was also demonstrated.

Case study #2 examined the efficiencies of wood-based biosorbents such as magnetite pine-bark (MPB), biochar (BC), and activated carbon (AC) at both lab and pilot scales. These biosorbents significantly reduced the concentration of pharmaceuticals in sewage effluent. The combined use of BC and MPB resulted in the simultaneous removal of various antibiotics from wastewater, with removal efficiencies ranging from 26% to 99.7% for different compounds. The enumeration of viable bacteria revealed that the regeneration of the BC-MPB bed with NaOH resulted in a drastic increase in bacterial counts in the treated water due to the desorption of adsorbed bacteria from the bed. The biotoxicity study using the *Nitrosomonas europaea* bioreporter strain revealed that the wastewater was generally non-toxic to this nitrifying bacterium and regeneration of pilot-scale column samples caused short-time toxicity just after the regeneration.

In case study #3, the effectiveness of two types of biochar in removing heavy metals and antibiotics via adsorption was explored. The adsorption capacities of biochars ranged from 58 to 75 mg of pollutant per gram of adsorbent, showing their suitability for sustainable removal of Pb^{2+}, Zn^{2+}, and sulfamethoxazole from wastewater. Additionally, photocatalysts (MnSBiOI and Sn_2VO_3) were tested for their ability to degrade antibiotics and contaminants of emerging concern (CECs) using visible light, achieving degradation efficiencies of over 80% for targeted antibiotics.

In the treatment of metal-rich effluents (case study #4), three Mannich-modified tannin-based coagulants (acacia, quebracho, and spruce tannin) were tested, with quebracho tannin showing high efficacy in removing vanadium. It achieved turbidity and vanadium removals above 88% across a wide pH range. The potential for Vanadium to co-select antibiotic resistance in metallurgical water was also explored with *Nitrosomonas europaea* bioreporter strain, revealing that the Vanadium did not exert significant selective pressure on aquatic bacterial communities.

One important objective of the REWA project (WP4) was to develop standardized protocols for microbiome analyses for risk-benefit assessments of bench- or pilot-scale water treatment technologies. Sampling in several Danish WWTPs and conducting various microbiological analyses led to the conclusion that *Aeromonas* spp. constitutes promising indicator organisms for water quality assessment and for evaluating water treatment impacts on AMR. Another WP4 case study indicated that water-treatment processes killing most microorganisms may lead to an increased prevalence of antibiotic resistance among the surviving bacteria. Hence, a polyphasic microbiome-directed approach will be needed to assess emerging water treatment technologies in order to evaluate risks for regrowth of bacteria surviving harsh water treatment processes. The ecological context of water treatment processes must also be considered in order to assess risks for environmental development and dissemination of antibiotic resistance from waste water treatment plants.

There were some delays in the progress of the project. One was due to the fire outbreak in the UKZN laboratory, which hindered the on-time implementation of experiments. The second delay was related to the closure of the laboratories in MIGAL due to the war in Israel. On the other hand, the synthesis and characterization of the adsorbents and the pilot-scale studies were completed as planned. The project also met its technological objectives by demonstrating the feasibility of these treatment methods for both pharmaceutical removal and metal-rich effluent treatment in real-world applications.

A key aspect of the project's success was its promotion of a multidisciplinary approach. The project integrated expertise from environmental engineering, chemistry, and microbiology. Collaboration between these fields was crucial in developing and testing the various adsorbents and coagulants and addressing the complex challenges posed by emerging pollutants and metal-rich wastewater. This multidisciplinary approach enabled the project to explore both the environmental and technical aspects of water treatment, making significant strides toward sustainable solutions. Also, collaboration was effective and well deepened throughout the implementation of the project.

Table of contents

Introduction

The increasing occurrence of antimicrobial resistance (AMR) and the persistence of contaminants of emerging concern (CEC) in water systems have become significant public health and environmental challenges. These pollutants, often originating from pharmaceuticals, personal care products, and industrial processes, pose a threat to aquatic ecosystems and human health. The proliferation of AMR, driven by the widespread use and disposal of antibiotics, further exacerbates these risks, potentially leading to the development of treatment-resistant pathogens.

This technical report presents the findings of the REWA project focused on the reduction and assessment of AMR and CECs in natural-based water treatment systems. The project intends to develop simple and sustainable technological solutions to combat antibiotic resistance in drinking water treatment and enhanced treatment of sewage and metal-rich effluents.

WP2 Material preparation and pilot design

This section summarises the methods used for synthesizing and characterizing the materials developed by the research partners in the REWA project. Also, the section gives a general description of the equipment and procedures employed in the pilot studies carried out during the project´s implementation. The main objective is to create sustainable materials for water purification, specifically targeting contaminants of emerging concern (CECs) to facilitate water reuse.

T2.1 Preparation of materials (MIGAL)

Biosorbents

Iron-modified peat and magnetite pine bark (MPB) biosorbents were prepared for the adsorption of antibiotics (levofloxacin and trimethoprim). To obtain iron for the iron-modified peat, 20 g of the crushed ferric groundwater treatment residual was dissolved in 1 L of HCl (1 M) and stirred for 3 h. The solution was filtered and purified using membrane filters, resulting in an iron sludge solution with 6750 mg/L iron concentration. Then, 32 g of peat was added in four batches to the iron sludge solution (with an initial iron concentration of 0.07 M). The mixture was stirred for 6 hours, with the pH maintained at 3 using a 10 M concentration of NaOH. After that, the mixtures were centrifuged in centrifuge bottles to separate the product from the iron solution. The iron-modified peat was washed with deionized water by the settling-decanting method several times until the supernatant was colourless with a pH of 7. Finally, the washed peat product was dried in the oven at 60 ˚C for 24 hours.

For the MPB, 9 g of sieved pine bark was soaked in 300 mL Milli-Q water under slow stirring. Meanwhile, 7 g $FeCl_3.6H_2O$ and 3.6 g-$FeSO_4.7H_2O$ were dissolved in 150 mL Milli-Q water. The iron solution and 1 M NaOH were added dropwise into the pine bark solution under stirring. The pH of the mixture was maintained at 9-10. The mixture was heated to 70°C for 3 hours, then washed with deionized water until clear and the biosorbent was dried at 60 ˚C for 24 h.

The biochar adsorbents used in this research were sourced from waste pine pallets and exotic plant materials (mainly bugweed). Both biochar materials were pyrolyzed at high temperatures, ground, and ball milled. The biochar derived from pine pallets is referred to as BCH 1, while that from exotic plant material is designated BCH 2. All sorbents underwent physical and chemical characterization using techniques such as X-ray diffraction (XRD), X-ray photoelectron spectroscopy (XPS), and Brunauer-Emmett-Teller (BET) surface area analysis, scanning electron microscopy (SEM), Thermogravimetric analysis (TGA).

Tannin-based coagulants

Three tannin raw materials, quebracho (*Schinopsis balansae*), acacia (*Acacia* mearnsii) and spruce (*Picea abies*) were tested for metal removal from industrial wastewater. Quebracho and acacia are commercial tannins and were supplied from SilvaTeam (Italy) and Serveyco (Spain), respectively. Meanwhile, spruce tannin was extracted from winter-harvested spruce trees from Northern Finland. The tannin-based coagulants were synthesized via aminomethylation using formaldehyde and ethanolamine. The process began by dissolving 2.5 g of tannin in water, raising the solution's temperature to 70°C, and adding 4.9 mL of ethanolamine. The pH was adjusted to 6.5, and the temperature was further increased to 80°C before gradually adding 1.38 mL of formaldehyde over 90 minutes. The reaction was completed by mixing at 85°C for 180 minutes. The product was stabilized by adjusting the pH to 1.6 and diluting it with water to a final concentration with a pH of ~2. The tannin samples were analyzed with XPS and electrospray ionization process (ESI) to elucidate their pristine characteristics, and the charge density of their modified coagulants was measured.

Photocatalysts

Manganese sulfide/bismuth oxyiodide (MSBI) nanocomposites for the photocatalytic degradation of tetracycline in this study. Firstly, manganese sulfide (MnS) was synthesized using a co-precipitation method. 1.9117 g of manganese acetate tetrahydrate and 0.8898 g of sodium sulfide were each dissolved in 60 cm³ of deionized water. The two solutions were mixed in a round-bottom flask, stirred for three hours at 80°C in an oil bath, and then transferred to a Teflon-lined stainless autoclave. The mixture was heated at 140°C for 20 hours. Afterwards, the precipitate was washed with deionized water and ethanol to remove unreacted materials and dried in a vacuum oven at 60°C for 12 hours. Bismuth oxyiodide (BiOI) was also prepared concurrently. For the BiOI composite, 2.43 g of bismuth nitrate was gradually added to 80 cm³ of ethylene glycol containing 0.51 g of potassium iodide (KI). The solution was stirred for 30 minutes at room temperature, then transferred into an autoclave and heated at 160°C for 12 hours. After cooling to room temperature, the precipitate was collected, centrifuged, and washed with ethanol and deionized water to remove impurities. Finally, it was dried in a vacuum oven at 60°C for 12 hours. Finally, the MSBi nanocomposites were synthesized using a mechanomixing technique by dispersing different masses of MnS and BiOI in deionized water. The mixtures were sonicated for 3 hours, stirred for an additional hour, and then centrifuged to remove water. The nanocomposites were dried in a vacuum oven at 60°C overnight, resulting in four distinct nanocomposites for further characterization.

Tin vanadate used for photocatalytic degradation of benzophenone-3 in the study was synthesized with both chemical precipitation and hydrothermal methods. For the chemical precipitation method, two solutions were prepared separately and labelled A and B. Solution A (2.29 g of tin (IV) chloride in water) was added dropwise to Solution B (0.76 g of ammonium vanadate in water) to form a pale yellow precipitate, which was stirred for 3 hours, washed, and dried at 70°C to obtain the tin vanadate powder. For surfactant-assisted synthesis, either CTAB or PEG 400 was added to Solution B before adding Solution A, followed by drying and calcining the mixture at 400°C for 4 hours, producing samples labelled SVC, SVP, and SVCTB, depending on the surfactant used. Tin vanadate was synthesized via a hydrothermal method using tin (IV) chloride pentahydrate and ammonium vanadate. The solution formed a yellow precipitate, which was stirred, washed, and transferred into an autoclave for 12 hours at 200°C. Surfactant-assisted versions were prepared by adding CTAB or PEG 400, followed by drying at 70°C and calcining at 400°C, with the hydrothermal tin vanadate labelled SVH and the surfactant-assisted samples labelled SVCTBH and SVPH, respectively, before being stored in vials.

T2.2 Pilot designs (MIGAL)

A device aimed at the removal of suspended materials in effluents was planned, as shown in Figure 1. The device is based on the use of clay-polymer coagulants. A small pilot was also tested *in vitro* for the removal of cyanobacteria from water sources. Additional information is described in Section T.3.1. The third demonstration device was developed, planned and built for the photodegradation of priority pollutants. The general scheme and a picture of the device are shown in Figure 2. The device was tested in synthetic and real effluents from "Shafdan" wastewater treatment plant. Additional information is described in Section T.3.1.
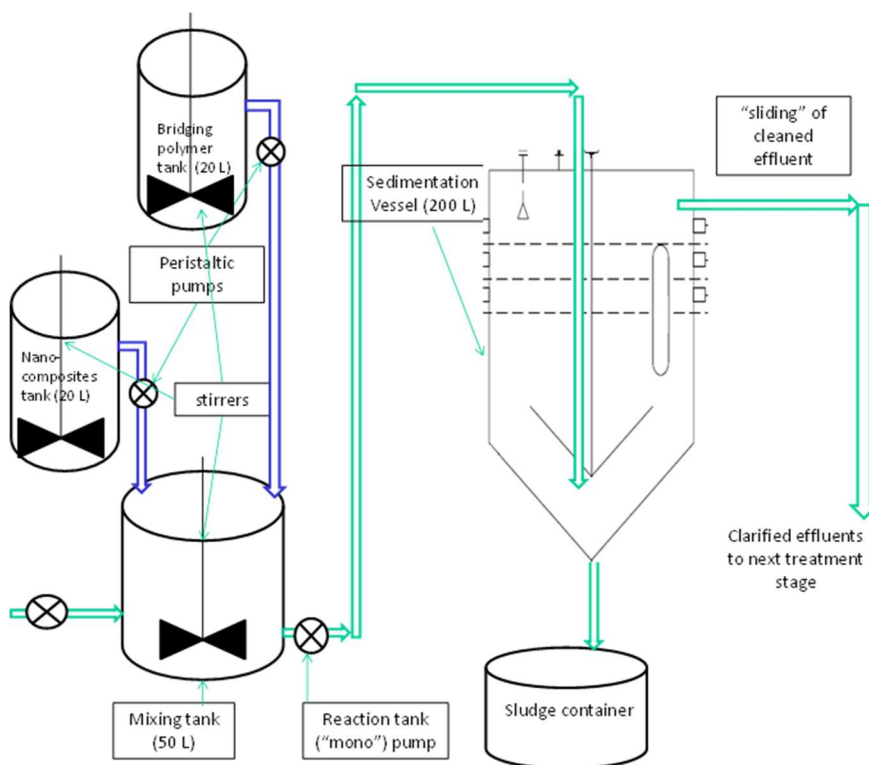
Figure 1. General scheme of a device for the removal of colloids and suspended solids in water sources
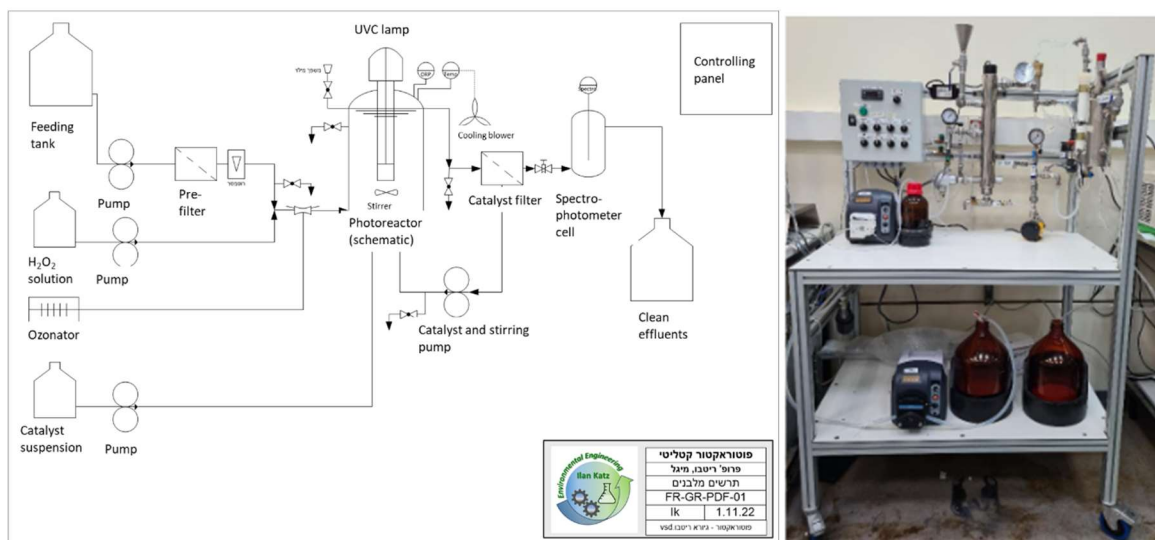
Figure 2. Schematic diagram (left) and photograph (right) of the photocatalytic degradation pilot

Two flow-through column studies (small-scale and pilot-scale) were performed to remove pharmaceuticals from municipal wastewater effluent. For the small-scale studies, columns with inner diameters of 6 cm and heights of 30 cm were used. The length of the column pipes of the pilot scale studies was about 120 cm with a 15 cm diameter and a volume of 21 L. A peristaltic pump was used to pump the effluent from the membrane bioreactor (MBR) basin to the columns from the top, and samples were collected from the bottom. Figure 3 shows the set-up of the column during the pilot-scale studies.
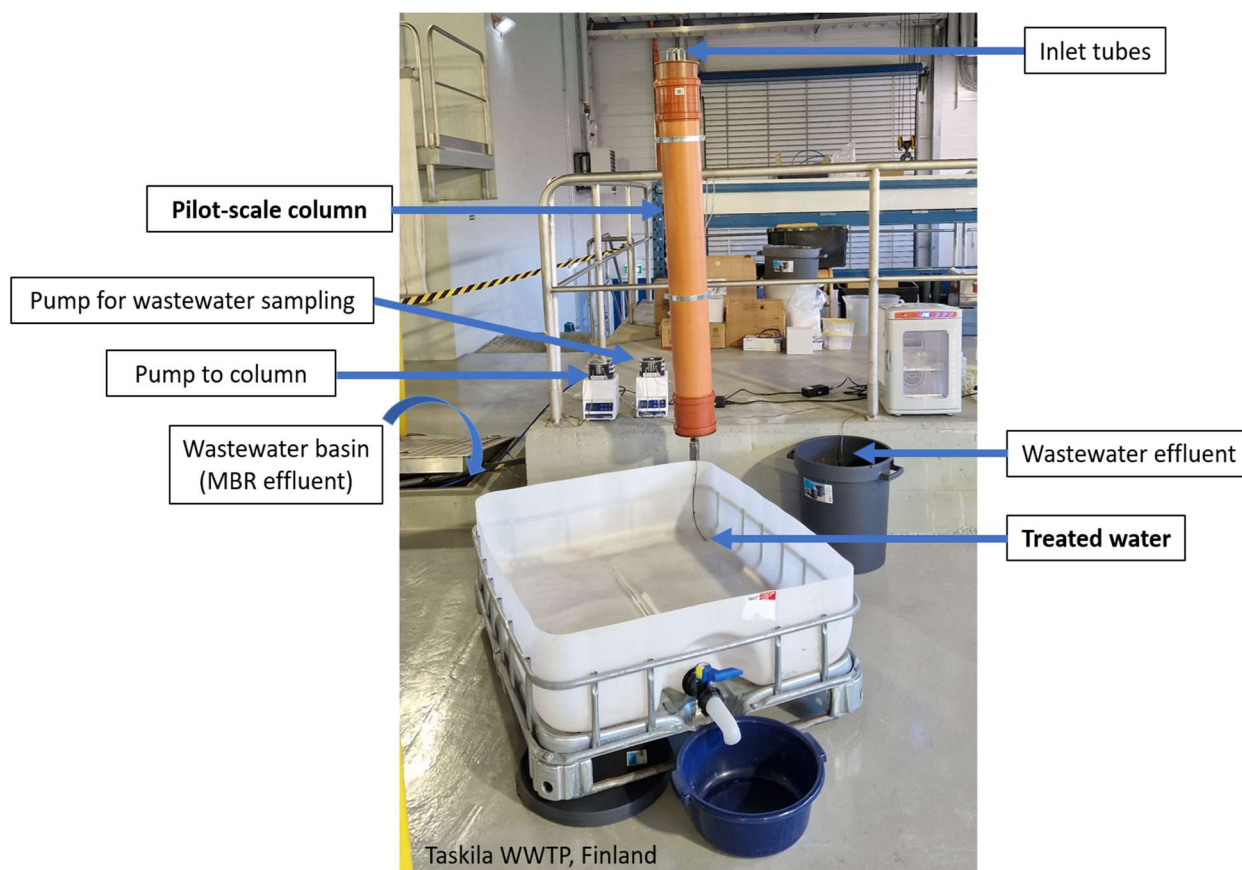
Figure 3. Set-up for the column of the pilot-scale studies

WP3 Demonstration

T3.1 Case study #1, surface water treatment (MIGAL)

Carbamazepine removal by clay-based materials using adsorption and photodegradation

Carbamazepine (CBZ) is one of the most common emerging contaminants released to the aquatic environment through domestic and pharmaceutical wastewater. Due to its high persistence through conventional degradation treatments, is considered a typical indicator for anthropogenic activities. This study tested the removal of CBZ through two different clay-based purification techniques: adsorption of relatively large concentrations (20-500 µmol L^{-1}) and photocatalysis of lower concentrations (<20 µmol L^{-1}).

The adsorption was tested as described in subsection on five clay-based adsorbents, including 3 raw clays: (bentonite, Ca- SWy1, and b) sepiolite), and 2 organoclay modified by benzalkonium and thiamine (bent-bzk and bent-B1). The adsorption isotherms were also described by the Langmuir adsorption model, and the parameters Smax and KL were evaluated. Organoclay based on BZK exhibited the lowest adsorption, whereas raw bentonite and Ca-SWy-1 adsorb more than 0.5 mmol g^{-1}. Such an effect is unusual since smectites usually have a low affinity to non-charged organic molecules. However, it should be emphasized that at low CBZ concentrations, adsorption to those clays is almost zero (see Figure 4b , which shows adsorption isotherms at low CBZ concentrations), yielding an "S-type isotherm". This indicates that the direct interaction between the clay surface and the pollutant is low, and only after obtaining some coverage of the clay surface, does adsorption increase. On the other hand, bent-B1 maximum adsorption is lower (app. 0.25 mmol g^{-1}, see Figure 4a) but it is also very efficient at low concentrations (see Figure 4b). The affinity of carbamazepine to bent-B1 increased considerably as demonstrated also in a higher calculated KL value.

a)   b)
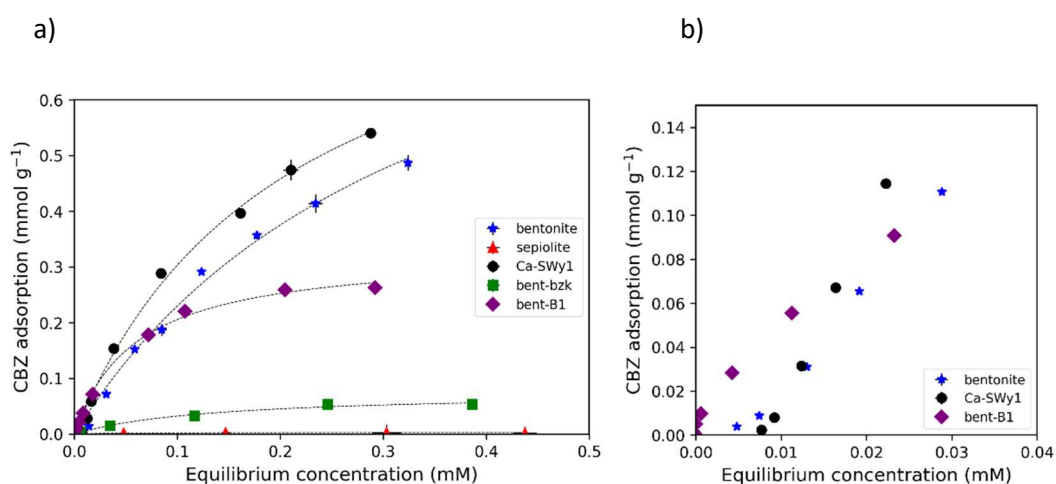
Figure 4. (a) Adsorption isotherms of carbamazepine on bentonite (blue asterisk), sepiolite (red triangle), Ca-SWy1 (black circle), bent-bzk (green square), and bent-B1 (purple diamond). Error bars represent triplicate standard deviations. The dashed lines represent Langmuir model predictions according to the estimated parameters detailed in Table 2. (b) Isotherms at low concentration of carbamazepine on bentonite, Ca-SWy1, and bent-B1

The sorption mechanism was examined by FTIR measurements, exchangeable cations released, and colloidal charge of the adsorbing clay materials. FTIR spectra of dried CBZ-clays were measured using an ATR device in order to confirm and evaluate the adsorption of carbamazepine on the absorbent particles by identifying the relevant structural group in the measured samples, whereas CBZ degradation will lead to different functional group vibrations. Figure 5a shows the spectrum of CBZ, raw bentonite, and CBZ-bentonite at several carbamazepine amounts. CBZ-bentonite samples exhibit five absorption bands that were not observed in raw bentonite, at approximately 1640, 1570, 1490, and 1460-1435 cm^{-1}. Those absorption bands were correlated to typical peaks of functional groups of CBZ, as observed in the carbamazepine spectrum sample, and are known from the literature (Kumar & Umamaheswari, 2011). The only absorption band in raw bentonite in this region is at ~1630 cm^{-1} and ascribed to the O-H deformation of hygroscopic water (Madejová & Komadel, 2001). While the three CBZ absorption bands in the range 1400-1500 cm^{-1} (ascribed to C=C vibrations) are in almost the same place for adsorbed and raw CBZ, bands ascribed to C-N bond (at app. 1600 cm^{-1}) and to the amide group (NH_2 scissoring/C=O stretching, at ~1670 cm^{-1}) appear shifted to lower energies. This may indicate that the interaction between CBZ molecules and the clay is via the amide group. An increase in all absorption bands in the range 1400-1700 cm^{-1} is observed according to the adsorption process as measured in the experiment (Figure 2a). Relative quantification of the CBZ absorbed can be performed by calculating the ratio between the intensity or the area of CBZ absorption bands, to that of the structural O-H band related to the clay at 3620 cm^{-1}, where CBZ has no absorption at all. Subsequently, those ratios were compared to the amount of carbamazepine adsorbed to the clay as measured in the previous adsorption experiment (Figure 5). Figure 5b represents the comparison of two normalized absorption bands to the adsorption results, including the absorption bands' height at 1490 and their area at 1460-1435 cm^{-1}. The linear correlation (R2>0.99) between the two data sets confirms the adsorption process as the reason for CBZ decrease in the equilibrium solution.

a)   b)
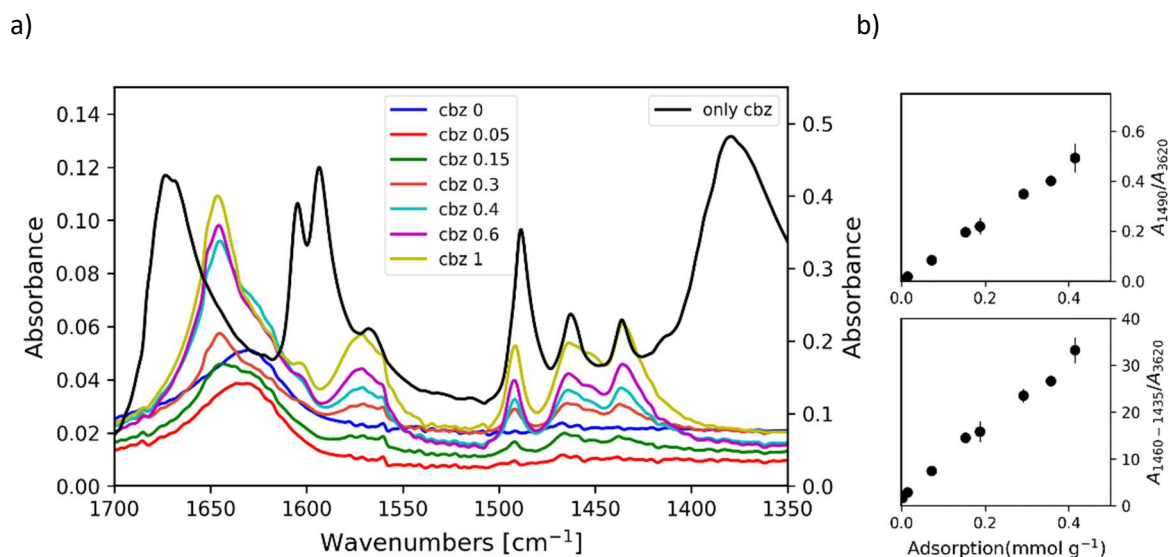
Figure 5. (a) ATR-FTIR spectra of CBZ (black, OD values on the right axis), bentonite raw clay (blue), and bentonite with added CBZ (in mmol g-1) as denoted in the legend (OD values on the left axis). (b) normalized absorption bands height at 1490 and area at 1460-1435 cm^{-1} compared to the adsorption results as measured by the mass balance during the adsorption experiments

In previous studies (Rytwo et al., 2024; Rytwo & Zelkind, 2022)we have shown that a combination of low concentrations of both heterogeneous and homogeneous catalysts may yield synergistic effects and speed up the photodegradation of priority pollutants such as BPS or ofloxacin.To test this effect on CBZ, we performed photodegradation experiments of a 21.2 μM (5 mg L^{-1}) CBZ solution, under UV irradiation, with a low concentration (0.2 mg L^{-1}) of the heterogeneous catalysts, at two hydrogen peroxide levels: (a) high (2.0 mg L^{-1}) and (b) low (0.5 mg L^{-1}). At 2 mg L^{-1} H$_2$O$_2$ concentration (results summarized in Table 1 and presented in Figure 6) the homogeneous catalyst already yields low t$_{1/2}$ values of less than 8 min. The addition of clays as heterogeneous catalysts makes almost no difference. As for TiO$_2$- it should be emphasized that when added alone at a low concentration (0.2 mg L^{-1}) almost no degradation is observed (Table 1), but the combination with 2.0 mg L^{-1} H$_2$O$_2$ slightly speeds up the process (t$_{1/2}$ changes from 6.4 to 5.9), and a small change in the pseudo- order is observed. At a low homogeneous catalyst concentration of 0.5 mg L^{-1}, the influence of all heterogeneous catalysts is significant: While with no heterogeneous catalyst t$_{1/2}$ at that hydrogen peroxide amount is about 219 min, the addition of 0.2 mg L^{-1} of TiO$_2$, barasym or laponite lowers t$_{1/2}$ to 68.0, 33.2 and 37.0 min, respectively. Pseudo-order also changes, especially for the clay minerals.

Table 1. Pseudo-orders and half-life times for photodegradation experiments.

Heterogeneous catalyst		H$_2$O$_2$ (mg L^{-1})	Pseudo-Order n_a	Half-Life t$_{1/2}$ (min)
Type	(mg L^{-1})			
None	0	0	0	212.1 ± 1.56%
		0.5	0	219.3 ± 2.77%
		1.0	0.76 ± 4.31%	15.6 ± 0.62%
		1.5	0.93 ± 3.39%	11.4 ± 0.89%
		2.0	1.01 ± 2.65%	7.60 ± 1.00%
		2.5	0.82 ± 2.13%	6.39 ± 0.85%
TiO$_2$,	0.2	0	0	189.31 ± 2.53%
	0.4	0	0	122.2 ± 1.97%
	1	0	0	120.7 ± 2.66%
	0.2	0.5	0	68.0 ± 0.86%
	0.2	2.0	0.90 ± 3.10%	5.90 ± 1.39%
Barasym	0.2	0	0	296.7 ± 1.68%
	1.0	0	0	215.9 ± 1.74%
	0.2	0.5	1.24 ± 5.24%	33.2 ± 0.41%
	0.2	2.0	0.84 ± 1.99%	6.90 ± 0.92%
Laponite	0.2	0	No degradation	-
	1.0	0	No degradation	-
	0.2	0.5	1.04 ± 4.27%	37.0 ± 0.54%
	0.2	2.0	0.82 ± 3.27%	6.80 ± 1.03%
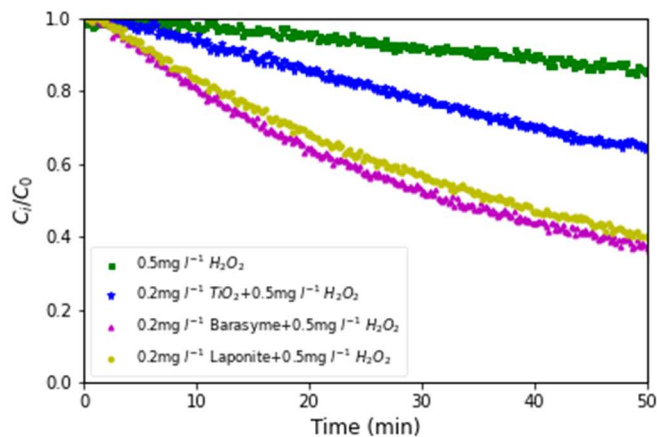
Figure 6. Photodegradation of a 21.2 µM (5 mg L^{-1}) carbamazepine under UVC irradiation, with 0.5 mg L^{-1} H$_2$O$_2$ alone or combined with 0.2 mg L^{-1} TiO$_2$, barasym or laponite

Quercetin-based adsorbent for zinc removal from mining effluent

Quercetin was found as an effective chelator to several metal ions affecting the bioavailability, speciation and toxicity of those metals in the human body. Therefore, we hypothesize that quercetin-based adsorbents can serve as an efficient alternative for treating zinc-rich effluent, selectively adsorbing zinc ions.

Adsorption experiments were conducted to evaluate the adsorption of quercetin on granular activated carbon (GAC) and powdered activated carbon (PAC) (Figure 7). The experiments revealed a high adsorption affinity of quercetin for both types of activated carbon. The adsorbent concentration of 0.8 mmol/mg was selected and used in all subsequent experiments. To ensure the removal of non-strongly bound modifiers from the adsorbent complexes, the washing process was performed over three cycles.
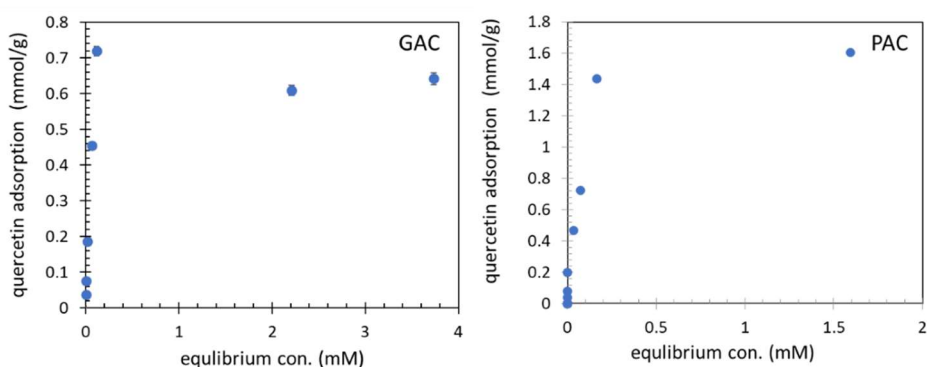
Figure 7. Quercetin adsorption isotherms on granular activated carbon (GAC), and powder activated carbon (PAC)

To evaluate the performance of modified and non-modified activated carbon in removing zinc ions, a series of adsorption experiments were conducted. The experiments assessed the adsorbent's capacity under conditions relevant to industrial effluent treatment. The study included testing the adsorption of zinc ions at varying concentrations onto both powdered activated carbon (PAC) and granular activated carbon (GAC), in their modified and non-modified forms. The experiments utilized a background solution designed to simulate the original mining effluent. The results, summarized as

adsorption isotherms (Figure 8), demonstrated the relationship between zinc concentration and the adsorbent's capacity.

For powdered activated carbon, the maximum adsorption capacity (Smax) was not significantly affected by the modification, with similar Smax values observed for both non-modified PAC and quercetin-modified PAC (PAC-que). However, a significant difference was observed in the lower concentration range, where PAC-que demonstrated a higher affinity for zinc ions. Complete zinc removal was achieved in this low adsorption range (up to 1 mg/g) with the modified PAC, whereas the non-modified PAC exhibited only partial adsorption. These findings highlight the enhanced selectivity of quercetin-modified PAC for zinc, particularly at low concentrations. In contrast, the results for granular activated carbon revealed a more significant effect of modification. The quercetin-modified GAC exhibited both a higher maximum adsorption capacity (Smax) and an increased affinity for zinc compared to its non-modified form. Overall, while both adsorbents showed benefits from quercetin modification, the granular activated carbon demonstrated greater overall improvement, making it a more promising candidate for large-scale water treatment processes.

a)   b)
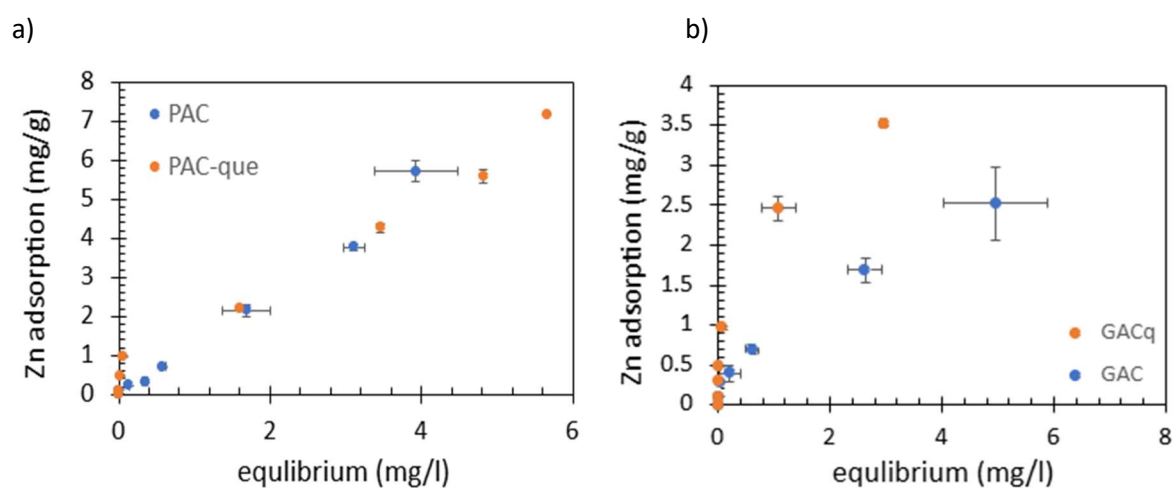
Figure 8. Zinc adsorption isotherms on (a) powder activated carbon in the modified (PAC-que) and non-modified (PAC) form; and   (b) granular activated carbon in the modified (GAC-que) and non-modified (GAC) form

Kinetic experiments were conducted to evaluate the adsorption rate of zinc ions using real wastewater spiked with 8 mg/L of zinc. Zinc concentrations were monitored at several time intervals following the addition of both modified and non-modified adsorbents. The results (Figure 9) showed an increased adsorption rate for the quercetin-modified PAC compared to its non-modified form. The difference in adsorption rate observed between the modified and non-modified GAC during the kinetic tests was less significant. suggests that, unlike PAC, the modification may not significantly enhance the kinetics of zinc adsorption for granular adsorbents under the tested conditions. Additionally, manganese concentrations were monitored during the experiment (Figure 10). The results indicated a notable improvement in adsorption rates for the modified adsorbents.
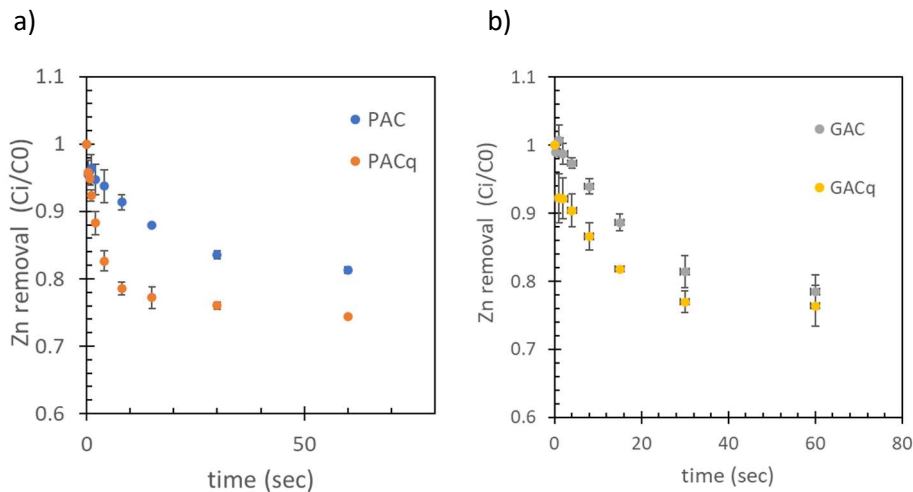
Figure 9. relative zinc adsorption over time with (a) modified and non-modified powder activated carbon and b) modified and non-modified granular activated carbon.
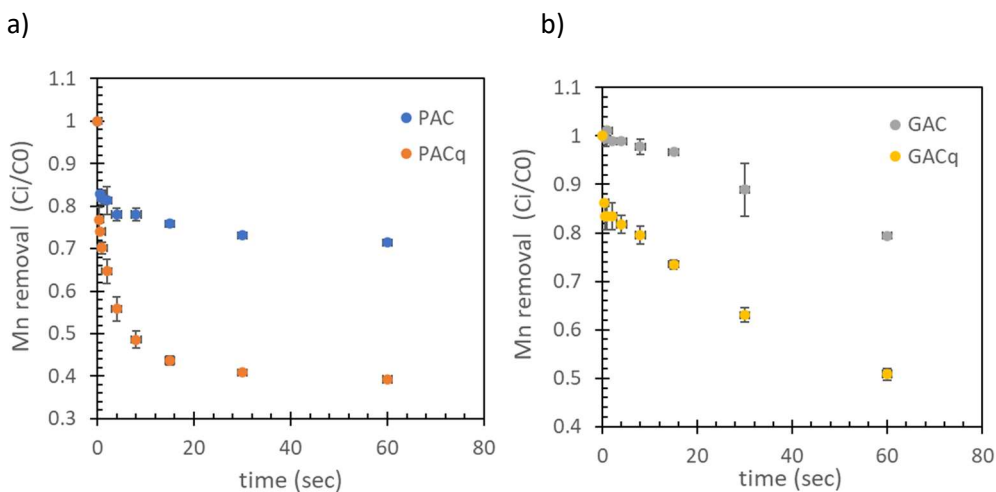
Figure 10. Relative manganese adsorption over time with a) modified and non-modified powder activated carbon and b) modified and non-modified granular activated carbon

Cyanobacteria removal

As a result of global warming processes and an excess of nutrients, mainly phosphorus and nitrates, which originate from chemical fertilizers and nutrients that are washed into water bodies, there is an increase in the primary production of algae, cyanobacteria (cyanobacteria) and aquatic plants. Cyanobacteria blooms are a global problem in surface water bodies, mainly due to their ability to produce toxins with a wide range of action and health effects on humans and animals. There is an increase in the number of reports of the presence of cyanobacteria in drinking water sources, and therefore there is a growing concern about the appearance of multiple cyanobacteria rashes that affect the quality of the water. Many studies are being done in order to understand the correct and most effective way to remove these microorganisms and their toxins in the processes of drinking water treatment. The purpose of this study is to test the effectiveness of the removal of cyanobacteria microcystis cells by physico-chemical means during different stages of culture growth. The study used clay-based composites, 20% DKG20 nanocomposites (0.6 g polydadmac per 1 g kaolinite) and 1% NC24 (1.8 grams of polydadmac to 1 gram of sepiolite) and raw polydadmac. The experiments examined the relationship between the growth stages, the amount of cell charges, and the concentration of flocculant material required to achieve maximum efficiency. The findings showed that a relationship

was found between the age of the culture and the amount of charges measured, and as the age of the culture increased, so did the number of charges of the cells. It seems that there is a significant difference in the number of charges per single cell in the early growth stages and the later stage, and that the relationship between the number of charges and the growth stage is not linear in terms of two orders of magnitude between the exponential growth stage and the stationary stage. In shading efficiency tests using the coago-flocculation process, it was found that at the beginning of the exponential growth stages, shading percentages above 80% were observed, with an upward trend up to the optimal point and then a decline. At the end of the exponential growth phase, good efficiency was observed at relatively low concentrations, followed by a gradual decrease in high concentrations, and in the stationary phase, a trend of increase was observed until the maximum concentration of DKG20 (84.05% (2.4[mg/L]), 83.75% (8.4[mg/L]), NC24 and polydadmac (85.48% (6[mg/L]), followed by a decrease in efficiency due to excess flocculant and a possible phenomenon of sign reversal. Especially in the early stages, and the percentage of rescues throughout the process was high. For NC24, higher concentrations were required to reach maximum shading percentages and Polydadmac showed similar results to NC24, with good efficacy at relatively high concentrations. In most of the growth stages, the actual observed optimal concentrations were lower than the concentrations theoretically calculated on the basis of PCD measurements, while in the early stages, the nanocomposite materials (NC24, DKG20) showed a better match between calculated and observed values, and in the later stages, all materials showed high efficiency at significantly lower concentrations than calculated. The findings emphasize the need for a tailored and dynamic approach to treating cyanobacteria blooms in water bodies, taking into account the type, growth stage of the population, and an informed choice of the type and concentration of the flocculant material. Figure 11 exhibits the floc formation and clarification achieved by increasing doses of DKG compared to the raw effluents ("0"). As can be seen, at high doses inefficient effect is observed apparently due to charge reversal.
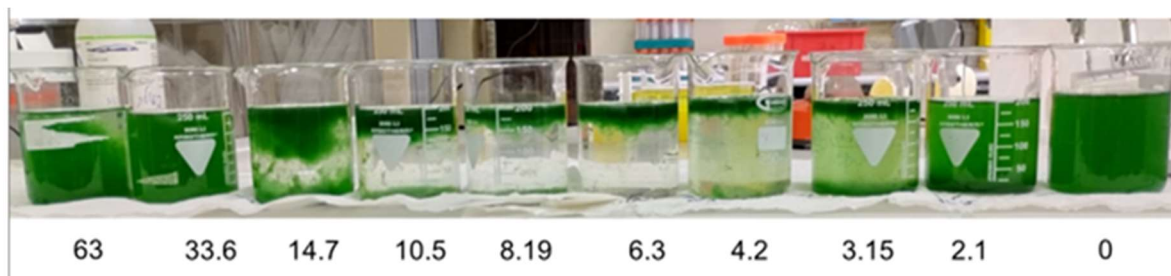
Figure 11. Cyanobacteria removal

The efficiency of the treatment on the formation of cyanobacteria flocs was confirmed by documenting the results in an inverted light microscope (Oberkochen, Germany) (AxioObserverZ1, ZEISS), used to examine cell and tissue cultures by way of reflection and transmission of light.Figure 12 shows an even distribution of the microcyst cells in the control sample. Initiation of cell association at DKG20 low concentrations is observed, consistent with 81.67% turbidity removal. Darkerflocs are observed with the increase in the added concentration up to 4 mg/L. At higher concentrations flocs are smaller, indicating the possibility of over-dosing or cell damage and the release of intracellular material of the cyanobacteria. NC24 at a concentration of 1.4 mg/L forms single flocs but also "loose" cells indicating limited efficacy, that improves at a concentration of 4.2 mg/L reaching an optimum at 7 mg/L, while flocs became smaller at 14 mg/L, but increased again at 22.4 mg/L. Such behavior may imply a more complex mechanism of action than simple charge neutralization. Raw polydadmac exhibits smaller and lighter flocs than the clay-polymers, and also a need for higher concentrations for effective action.
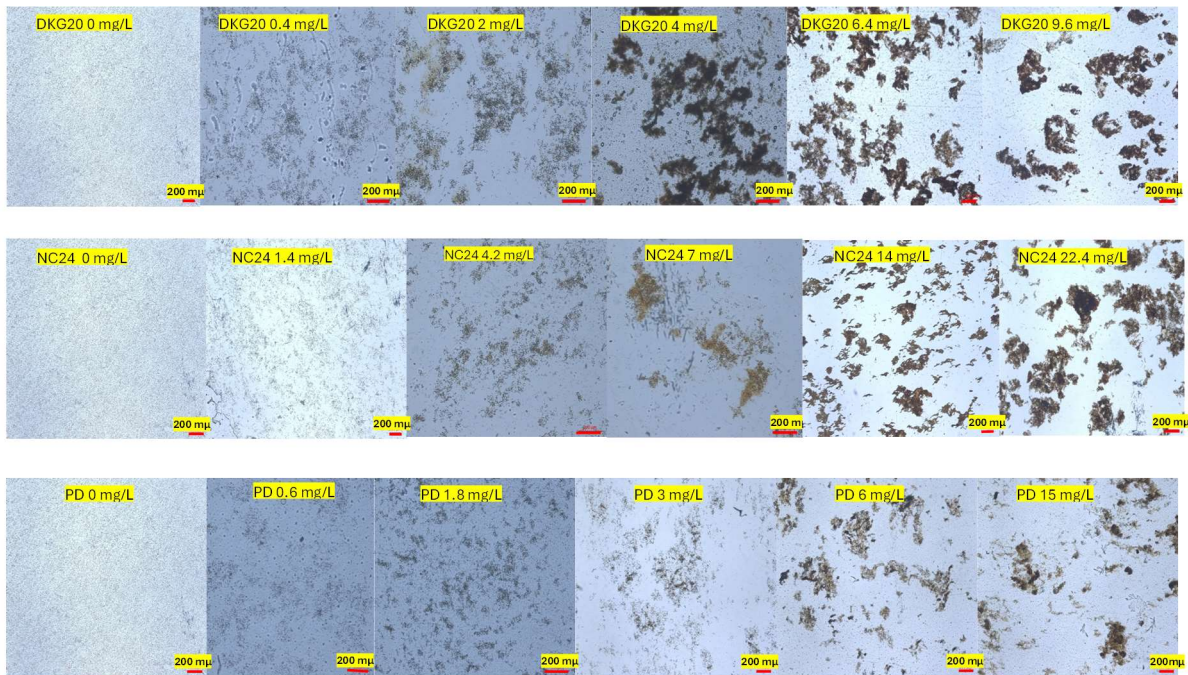
Figure 12. Inverted light microscope samples of clay polymer (DKG and NC) and raw polymer (PD) cyanobacteria suspensions

In summary- clay polymer coagulants appear to present very effective materials for the clarification of cyanobacteria polluted water sources, however additional research about possible release of toxins due to cell fracture is ongoing.

It should be noted that the original plan was to deploy a full pilot aiming removal of algae from water from natural sources. The scheme (shown in Figure 1 in section T2.2.) presents the general structure of such pilot, that was partly constructed. However, due to the situation and event in our region (Northern Israel) the pilot constructed was adapted to the clarification of olive mill effluents, and is indeed still in use, attached to a anaerobic reactor that reduces the chemical oxygen demand of the effluents. The pilot achieves a more than 97% suspended solids removal.

Photodegradation studies using the photocatalysis device

Figure 2 in section T2.2 presents the scheme and a photo of the photocatalysis device aiming removal of contaminants of concern (CECs). The device was tested with a number of contaminants (carbamazepine, acesulfame and iohexol. The test results were inconclusive, but on the other hand, the work on the device shows the decomposition of part of the contaminants tested.

Preliminary Tests: A 4-liter solution was prepared in twice distilled water of CBZ, IXL and ACE (each substance separately) at a concentration of 0.25 mg/L in a vessel wrapped in foil to prevent the penetration of light. To CBZ and IXL solutions, 0.075 millimolar hydrogen peroxide was added. The solutions were poured into the dispenser until droplets were observed coming out of the measuring tube, after which the flow was stopped. The flow rate was changed to 30 RPM, the UVC light was turned on, and the measurement began at different points in time, in the next range of 0-40 minutes. At any point in time, 1 mL is pumped into vials that were measured by an LC-MS. For each material, a

calibration curve was created by which the concentrations in the various samples could be calculated. A similar experiment was performed with a mixture of the pollutants.

Test on water from "Shafdan" wastewater treatment plant: The concentrations of contaminants CBZ, IXL and ACE in tertiary and pre-chlorinated effluents were measured by LC-MS in two experiments. Following that, experiments were performed with the activation of the UVC bulb, and in another experiment with the activation of the UVC lamp and the presence of hydrogen peroxide at a concentration of 0.075 millimoles. The concentrations of contaminants were sampled from the system for about 28 minutes, every few minutes, and measured by LC-MS. In addition to that experiments were performed on tertiary Shafdan water, with the spiking of CBZ, IXL and ACE (each substance separately) at concentrations of 0.3, 1, and 1 mg/L respectively in a heat bottle to prevent light penetration. To the solutions of CBZ, IXL 0.075 mM hydrogen peroxide was added. Flow rate through the device was calibrated until an increase was observed at a pressure of about 0.5 bar, and then an outlet tap of the water from the system was opened, while maintaining a pressure of 0.5 bar in the system. The UVC light was turned on and the measurement began at different points in time, in the next range of 0-28 minutes from the measuring booth. At any given point in time, 1 mL was pumped into dark vials taken for measurement in LC-MS. An additional test was performed was tertiary Shafdan water spiked with a mixture of CBZ, IXL and ACE (all ingredients together) at 0.3, 1, and 1 mg/L, and hydrogen peroxide was injected into the solution at a rate equivalent to 0.075 mM. The UVC light was turned on and the measurement began at different points in time, in the next range 0-28 minutes from the measuring booth. At any given point in time, 1 mL was pumped into brown HPLC bottles taken for measurement in LC-MS.

Results for the experiment with raw Shafdan water and the separated spiked pollutants is shown in Figure 13. It can be seen that CBZ is not well degraded by the system (Figure 13a), whereas ACE (Figure 13c) and IHX (Figure 13b) are removed after less than 10 minutes. Some degradation of CBZ is observed in the raw effluents (Figure 13d), but the process is very slow. ACE is not present in the raw effluents, and IHX is observed but rapidly degraded. Results similar to those presented in Figure 13d were measured for the Shafdan water spiked with a mixture of effluents, indicating that the device works very well for ACE and IHX, however for CBZ additional improvements must be applied, for example – addition of a mineral catalyst or processes based on adsorption matrices, as described in "Carbamazepine removal by clay-based materials using adsorption and photodegradation" section in part T.3.1.
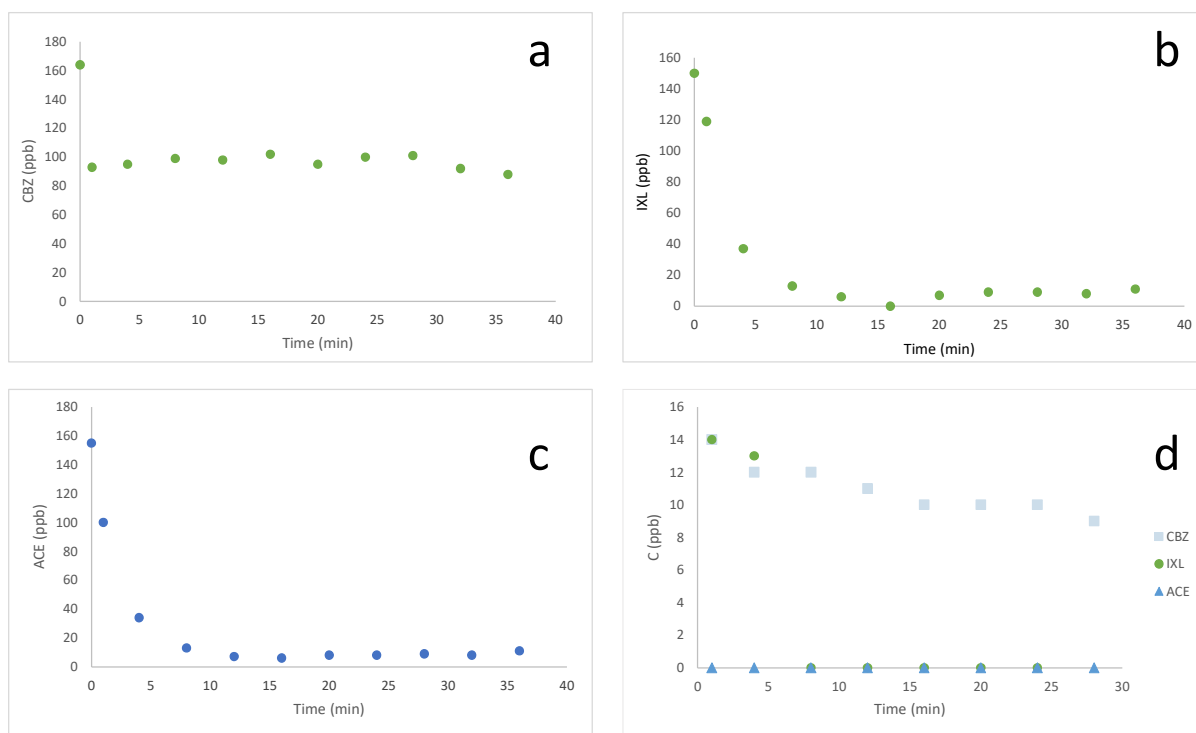
Figure 13. Results for the experiment with raw Shafdan water

T3.2 Case study #2, sewage effluent treatment (UO)

In case study #2, the adsorption capacity of iron-modified peat and magnetite pine bark (MPB) for levofloxacin and trimethoprim removal from synthetic solutions and municipal wastewater effluent was first performed. The results from the of antibiotics adsorption by iron-modified peat and magnetite pine bark has been published (Mohammadzadeh & Leiviskä, 2023). In brief, both biosorbents effectively removed levofloxacin and trimethoprim from synthetic solutions. The adsorption of levofloxacin was little influenced by pH compared to trimethoprim. The equilibrium removal efficiency of antibiotics over both biosorbents was reached after 180 min contact time. The maximum adsorption capacity over iron-modified peat was about 200 mg/g for both antibiotics and over magnetite-pine bark 153.0 mg/g for levofloxacin and 184.1 mg/L for trimethoprim. Experiments with real wastewater effluent revealed trimethoprim removal of 56.6–84.3% (dosage: 3 g/L). Moreover, a variety of other pharmaceuticals were removed by biosorbents. Then batch experiments and column studies were performed with the sewage effluent. The small-scale column study compared MPB to activated carbon (AC). Both adsorbents were mixed with biochar (BC) as MPB has a small particle size. Column study lasted 2 months. Batch experiments were conducted to verify the effect of each adsorbent alone. In the pilot-scale study, one bigger column was filled with MPB-BC mixture and used to treat the same wastewater effluent for four months. The results of these experiments will be summarized below, while the scientific articles will contain detailed results (Mohammadzadeh et al., 2025).

Batch Experiments

The pharmaceutical analysis of wastewater effluent (WW) after batch adsorption using AC, BC, and MPB sorbents revealed varying levels of removal efficiency (Table 2). AC demonstrated the highest efficiency, reducing most pharmaceutical concentrations to below detection limits. MPB also showed significant removal, with efficiencies ranging from 10.5% (ketoprofen) to 82.2% (trimethoprim). BC

had the lowest removal rates, with efficiencies ranging from 10.3% (amisulpride) to 61.8% (candesartan), and it failed to remove certain pharmaceuticals like O-Desmethylvenlafaxine and clarithromycin.

Table 2. Pharmaceutical analysis results of batch shaking via AC, BC, and MPB with municipal wastewater effluent (WW).

Pharmaceuticals	WW (μg/L)	AC (μg/L)	BC (μg/L)	MPB (μg/L)
Antipsychotics				
Amisulpride	0.29	<0.01	0.26	0.054
Antibiotics				
Azithromycin	0.078	<0.01	0.069	0.019
Clarithromycin	0.015	<0.01	0.015	0.01
Clindamycin	0.14	<0.01	0.12	0.11
Metronidazole	0.16	<0.020	0.14	0.14
Piperacillin	0.062	<0.01	0.088	0.026
Roxithromycin	0.012	<0.005	0.012	0.008
Benzotriazole	1.9	<0.04	0.96	0.91
Sulfadiazine	0.042	<0.01	0.035	0.03
Sulfamethoxazole	0.054	<0.010	0.037	0.019
Trimethoprim	0.41	0.006	0.36	0.073
Analgesics and NSAIDs				
Ketoprofen	0.029	0.006	0.11	0.026
Tramadol	0.56	0.011	0.44	0.22
Antiepileptics				
Lamotrigine	3.8	0.073	2.8	0.76
Beta blockers				
Metoprolol	0.28	<0.005	0.22	0.13
Benzodiazepines				
Oxazepam	0.45	<0.01	0.39	0.32
Antihistamines				
Cetirizine	7.7	0.15	6.3	2.5
Sedative-hypnotics				
Zopiclone	0.6	<0.02	0.56	0.11
Antidepressants				
Venlafaxine	0.72	0.029	0.62	0.28
O-Desmethylvenlafaxine	1.4	0.025	1.4	1.2
Antihypertensives				
Valsartan	3.6	0.13	2	1.7
Diuretics				
Hydrochlorothiazide	1.7	0.11	1.4	1.1
Angiotensin receptor blockers (ARBs)				
Candesartan	0.89	<0.05	0.34	0.24
Anticonvulsants				
Carbamazepine	0.18	0.006	0.15	0.13

Antibiotics were found to be in low concentrations in WW, ranging from 0.012 µg/L (roxithromycin) to 1.9 µg/L (benzotriazole). AC effectively removed all antibiotics except trimethoprim (0.006 µg/L). Trimethoprim, with an initial concentration of 0.41 µg/L, was well removed by both AC (98.5%) and MPB (82.2%), while BC achieved only 12.2% removal. MPB also effectively removed azithromycin (75.6%), though lower removal rates were seen for clindamycin (21.4%), clarithromycin (33.3%), and others. At the highest concentration in WW, Benzotriazole was moderately removed by MPB (52.2%) and BC (49.5%). MPB outperformed BC in removing sulfamethoxazole, with a 33.8% higher efficiency.

Besides antibiotics, MPB showed moderate removal of other compounds like carbamazepine (27.7%), hydrochlorothiazide (35.2%), and venlafaxine (61.1%). BC had lower removal rates for these compounds but was more effective at removing candesartan (61.7%) than other pharmaceuticals. Regarding water quality parameters, AC significantly reduced COD from 32.1 mg/L to 18.2 mg/L, while BC had minimal impact on COD (30.4 mg/L), and MPB slightly increased it to 44.4 mg/L. Phosphate removal was observed with both AC and MPB, while total nitrogen and pH levels remained largely unchanged after adsorption.

Column study

The pharmaceutical analysis from the small-scale column test revealed that cephalexin and clarithromycin were not detected in wastewater effluent or column samples. Regeneration did not significantly alter pharmaceutical concentrations, except for venlafaxine, which disappeared post-regeneration. Trimethoprim was commonly found in wastewater effluent (0.017-0.284 µg/L) but effectively removed in column samples. Levofloxacin, detected in two effluents, was mostly removed, with one higher value observed after MPB treatment. Metoprolol and tramadol were generally not found after adsorption, except in a few samples.

Venlafaxine, present in many effluents, was removed by AC but detected in low concentrations after MPB treatment, disappearing after further treatment. Furosemide and ibuprofen were fully removed across all columns, and carbamazepine was not detected post-adsorption, except for a few low concentrations. Losartan was mostly removed, though higher concentrations appeared in some BC+MPB samples post-regeneration. Diclofenac was reduced or undetected after adsorption. AC effectively reduced COD, while BC+MPB had little impact. Total nitrogen decreased slightly across all columns, phosphate levels increased after adsorption, and pH values rose post-treatment. Overall, the columns efficiently removed the analyzed pharmaceuticals.

Pilot study

The pilot-scale adsorption effectively removed a variety of pharmaceuticals from wastewater effluent. Many were present in low concentrations, often below detection limits. Antibiotics like azithromycin, clarithromycin, metronidazole, piperacillin, roxithromycin, and trimethoprim were significantly reduced, with trimethoprim removed. Sulfadiazine, sulfamethoxazole, and clindamycin also showed good removal efficiencies.

Beyond antibiotics, the pilot-scale adsorption has also effectively removed other drugs. For instance, blood pressure medications like furosemide and hydrochlorothiazide showed impressively high removal rates of 93.5% and 81.9%, respectively. Antipsychotic and anticonvulsant drugs, including amisulpride, quetiapine, and carbamazepine, were efficiently reduced. Antihistamines like desloratadine, fexofenadine, and cetirizine also demonstrated high removal efficiencies, with cetirizine reducing from 9.06 µg/L to 0.359 µg/L.

Painkillers such as naproxen and ibuprofen were effectively removed, with tramadol and ketoprofen achieving over 89% removal. Beta-blockers like metoprolol were also reduced to below detection

limits. Oxazepam, used for anxiety, was removed by 91.3%, while antifungal drugs like benzotriazole were removed entirely, though fluconazole showed only slight removal. Antidepressants such as venlafaxine and citalopram were also efficiently removed. Losartan and valsartan, used to treat high blood pressure, showed removal efficiencies of over 80%. Hormone treatments like bicalutamide were reduced to below detection limits, while epilepsy medication lamotrigine was removed by 97.7%. However, candesartan showed only a 26% removal efficiency. Caffeine and xylometazoline were partially removed, and zopiclone, used for insomnia, was significantly reduced.

While pilot-scale adsorption has proven effective for a wide range of pharmaceuticals over a four-month period, there is a clear need for further studies to optimize the treatment process. Although the contact time was high, previous research has suggested that shorter times could also be effective. However, it's important to note that COD, total nitrogen, and phosphate levels were slightly higher after treatment. The regeneration of the biosorbents with NaOH led to iron leaching from MPB, indicating the need for more research to optimize NaOH concentrations and minimize this effect.

T3.3 Case study #3, sewage effluent treatment (UKZN)

In task #3 biochar prepared from either waste pine pallets (BCH1) or cleared exotic plant material (BCH2), and photocatalysts based on bismuth oxyhalides or tin vanadate, were tested for their efficacy to adsorb or degrade CECs. This report provides a summary of the results found upon testing the materials. More details will be provided in scientific publications (currently in preparation).

Batch adsorption studies on the uptake of Pb^{2+}, Zn^{2+} and sulfamethoxazole onto two types of biochar

Biochar is obtained from the pyrolysis of biomass and is a form of charcoal. It is recognised that biochar is a promising adsorbent for the remediation of wastewater. Both organic and inorganic pollutants can be removed. The properties of the feedstock influence the behaviour of the biochar. In this work two biochars were tested: one was from waste pine pallets (BCH1) and the other was from exotic plant material that had been removed (BCH2).

Batch experiments were conducted to determine the effect of pH, contact time, adsorbate concentration, adsorbent dose, and temperature on the removal efficiencies. The contact time and temperature data were subsequently fitted into various kinetics and isotherm models to understand the underlying mechanisms. The equilibrium concentrations of Pb^{2+} and Zn^{2+} were determined by ICP-OES, while sulfamethoxazole (SMX) was determined by UV-vis spectrophotometry.

The effect of pH on the removal of the analytes was studied over the range of 2 to 12. A change in the solution pH influences the chemical behaviour of the adsorbates, the charges on the adsorbents, and the speciation of the metal ions in the solution. The uptake of Pb^{2+} and Zn^{2+} by the biochars was low at acidic conditions and increased as the solution pH increased. Further experiments were conducted at pH 5 and 6 for Pb^{2+} and Zn^{2+}, respectively. On the other hand, for SMX, the highest removal was observed under acidic pH conditions, where the amine groups are protonated, and decreased as the pH solution increased. Thus, for SMX, a pH of 2 was used for further experiments.

The mass of the adsorbent in batch experiments affects the adsorption capacity. The percentage removal increased as the adsorbent mass increased, which can be attributed to the increased number of available active adsorption sites, which enables an increase in adsorption efficiency. For Pb^{2+}, maximum removal was obtained with 40 mg of both biochar types, while for Zn^{2+} maximum removal was obtained with 35 mg of BCH2 and 50 mg of BCH1. In the case of SMX, maximum removal was achieved with 40 mg of BCH1 and 50 mg of BCH2.

For the effect of contact time, at the beginning of the adsorption, there was a rapid increase in the adsorption capacity because of the accessibility and availability of the active sites suggesting strong electrostatic interactions between the adsorbates and the adsorbents. After that, the adsorption was stable until equilibrium was attained when little or no increase in the adsorption capacity was observed. Equilibrium was achieved at 400 min with both adsorbents for all the adsorbates. Higher removal efficiencies were obtained with BCH1 for Zn^{2+}, while BCH2 showed better removal of Pb^{2+} and SMX.

It was found that the contact time studies were most accurately characterized by the pseudo-second-order kinetics model, except for Zn^{2+} removal onto BCH2, which was better described by the pseudo-first-order model. The pseudo-second-order model postulates that the rate-determining step is governed by chemisorption, a process in which valence forces are involved through electron exchange or sharing.

Generally, an increase in adsorption capacity was noticed with an increase in adsorbate concentration from 10 to 100 mg L^{-1}. An increase in the concentration of the adsorbate increases the driving force needed to overcome resistance on the active sites of the adsorbents.

The effect of temperature on the adsorption of Pb^{2+}, Zn^{2+}, and SMX onto BCH1 and BCH2 was studied between temperatures of 25 to 40 °C. The adsorption showed no significant change in the adsorption capacity as the temperature was changed. This shows that temperature does not affect the adsorption of Pb^{2+}, Zn^{2+}, and SMX onto the biochars. This trend suggests an endothermic process of adsorption for both metal ions and SMX.

Isotherm studies were performed to better understand the interactions between adsorbates and adsorbents. For Pb^{2+}, the Freundlich isotherm best described the removal by BCH2, while the Langmuir isotherm was considered the best-fit isotherm for BCH1. The Freundlich isotherm best described the removal of Zn^{2+} and SMX onto BCH1 and BCH2. The Langmuir isotherm postulates that the adsorption occurs on a homogenous surface with identical sites, each with the same heat of adsorption. In contrast, the Freundlich model proposes that adsorption happens on a heterogeneous surface and that the heat of adsorption decreases exponentially with surface coverage.

This work shows that both biochars can be used as potential adsorbents for the sustainable removal of Pb^{2+}, Zn^{2+}, and the antibiotic, SMX, from wastewater with good adsorption capacities ranging from 58 to 75 mg of pollutant to g of adsorbent.

Bismuth oxybromide/red phosphorus nanocomposites for the photocatalytic degradation of tetracycline by visible light

Bismuth oxyhalide-based compounds such as bismuth oxyiodide, bismuth oxychloride, and bismuth oxybromide have been gaining popularity because of their ability to absorb visible light. In this study bismuth oxybromide (BiOBr) was chosen for the photocatalytic degradation of a commonly used broad-spectrum antibiotic, tetracycline. However, BiOBr suffers from poor separation of the photogenerated electrons and holes, which impedes its ability to perform well as a good photocatalyst. To overcome this limitation, it was coupled with red phosphorus (RP) to form a heterostructure. Red phosphorus is a versatile element that is able to absorb visible light over a wide range. It is also stable, not toxic and inexpensive. Therefore, in this work, bismuth oxybromide/red phosphorus (BiBrP) composites were prepared by a facile hydrothermal approach.

RP performed poorly relative to BiOBr in the photodegradation of tetracycline with visible light. The composites demonstrated improved photocatalytic degradation efficiencies, with the 15% BiOBr/85% RP composite achieving the highest degradation efficiency of tetracycline (77%) in a period of 120

minutes. The improvement in the photocatalytic degradation ability of the composites could be attributed to the increased visible light absorption, which translates to more photons of light being absorbed by the composite.

The degree of mineralisation of tetracycline was measured by the total organic carbon (TOC) analysis. Based on the results it was concluded that 74% of the organic carbon was removed from the tetracycline solution with the remaining amount indicating the presence of reaction photoproducts.

In conclusion, the coupling of bismuth oxybromide and red phosphorus to form composites resulted in improved optical and electronic properties. The composites showed better light absorption in the visible range, and charge recombination was suppressed. Hence, these composites can be used in the degradation of emerging contaminants.

Bismuth oxyiodide/manganese sulfide nanocomposites for the photocatalytic degradation of tetracycline by visible light

Manganese sulfide (MnS) is a p-type semiconductor photocatalyst that has shown potential in applications such as in the fabrication of solar cells, environmental remediation, and H_2 generation as a result of its unique optical and electronic properties. However, the drawbacks of manganese sulfide are a wide bandgap and poor separation and transference of the charge carriers. On the other hand, bismuth oxyiodide (BiOI) is a semiconductor photocatalyst belonging to the family of bismuth oxyhalides. It has attracted much interest due to its good optical and electrical properties, non-toxicity, and low cost. It has also demonstrated excellent ability to perform photocatalytic degradation of pollutants. In this work, bismuth oxyiodide/manganese sulfide heterostructures were fabricated and tested on the photocatalytic degradation of tetracycline.

The photocatalysts showed good photocatalytic activity against tetracycline, with the 30% BiOI/70% MnS composite showing the highest percentage degradation of tetracycline (84%). This improved photocatalytic performance could be attributed to the narrow energy gap and good separation and transference of electron-hole pairs at the semiconductor interface.

The total organic carbon (TOC) analysis was performed to check the degree of mineralisation. After 300 minutes of reaction time, 90% of the total carbon content was removed. These results suggest that the tetracycline antibiotic had been converted to less harmful products under visible light in the presence of the 30% BiOI/70% MnS composite.

In conclusion, a bismuth oxyiodide/manganese sulfide heterostructure photocatalyst was successful in degrading approximately 84% of the initial tetracycline within a period of two hours. This activity was mainly attributed to the fast separation and transportation of electron-hole charge carriers. This work paves the way for novel photocatalysts that can be used to remediate polluted water systems.

Tin vanadate for the photocatalytic degradation of benzophenone-3 by visible light

Semiconductor photocatalytic degradation of organic pollutants is a reliable and sustainable environmental remediation technique. Tin oxide-based nanomaterials are one of the most widely studied semiconductors. Properties like non-toxicity, variable oxidation state, and cost-effectiveness make tin oxide suitable for this purpose. One advantage of this perovskite-like material is the hybridised valence band (VB) of the metal and oxygen, which causes a narrowing of the bandgap energy and enhanced mobility of charges.

The sizes, shapes, morphology, and activities of many photocatalysts have been altered by the use of surfactants during their synthesis. Hence, in this study, we synthesised a tin vanadate photocatalyst through six different synthesis conditions to enhance its optoelectronic and surface properties. The

synthesis methods were chemical precipitation, surfactant-assisted (PEG and CTAB) chemical precipitation, hydrothermal synthesis, and surfactant-assisted (PEG and CTAB) hydrothermal synthesis. The optical and electronic properties were examined, and the photocatalytic degradation efficiency was tested on a recalcitrant CEC, namely, the sunscreen filter benzophenone-3.

Tin vanadate prepared hydrothermally in the presence of the CTAB surfactant performed best, and at pH 3 it showed the highest degradation efficiency of 81.8%. The total organic carbon test (TOC) indicated a removal of 58.54%. The TOC result suggested that some organic compounds might not have been fully degraded after 300 min of photocatalytic degradation. Hence, a GC-MS method was utilised to identify the remaining organic moieties. The results show that benzophenone-3 was degraded into organic and inorganic fragments.

This study demonstrated that the Sn_2VO_3 photocatalyst prepared by the CTAB-assisted synthetic route could degrade benzophenone-3, a recalcitrant CEC, when exposed to visible light irradiation.

T3.4 Case study #4, metal-rich effluent (UO)

Performance of spruce and quebracho tannin-based coagulants to iron sulfate for removing vanadium from mine-impacted water

The study evaluated the effectiveness of spruce and quebracho tannin-based coagulants in comparison to iron sulfate for removing vanadium from water impacted by mining activities. Conducted by the University of Oulu in collaboration with the University of KwaZulu-Natal, the research was published in the *Chemical Engineering Journal* under the title "*Vanadium removal and floc characteristics of tannin biocoagulants and iron sulphate in the treatment of mine effluent*" (Bello et al., 2023). Spruce tannin was sourced from winter-harvested spruce bark and extracted using a sequential cold- and hot-water method, while the quebracho tannin was commercially supplied by the Silva team in Italy. Both tannin samples were cationized through the Mannich reaction using ethanolamine as the nitrogenating agent. The iron sulfate used in the study was provided by Kemira Oyj, located in Helsinki, Finland.

The mine water sample was obtained from the Mustavaara mine in Northern Finland—an inactive open-pit mine rich in vanadium, titanium, and iron deposits. The effluent was studied at the natural pH (7.4) and adjusted pH levels of 4 and 9. With the use of the MINEQL+ program, a theoretical equilibrium of vanadium (V) species in the mine water at various pH values was established. This demonstrated that at pH >3, V(V) species exists primarily as anions. Prior to testing, the charge densities of the tannin-based coagulants at pH values of 4, 7, and 9 were measured. Results indicated that the spruce tannin coagulant exhibited charge densities of 3.18 ± 0.04 meq/g at acidic pH, 1.95 ± 0.04 meq/g at neutral pH, and -0.46 ± 0.20 meq/g at alkaline pH. In comparison, quebracho tannin demonstrated relatively higher cationic charge densities of 4.06 ± 0.01 meq/g at pH 4, 2.28 ± 0.05 meq/g at pH 7, and 0.19 ± 0.05 meq/g at pH 9.

The coagulation experiment results demonstrated that the quebracho tannin coagulant achieved impressive turbidity and vanadium removal rates, exceeding 88% across a wide pH range. In comparison, the spruce tannin coagulant showed better vanadium removal at pH 7.4 (46%) and pH 4 (70%) but was less effective at pH 9, with a removal rate of 39%. This reduced efficiency at alkaline pH was attributed to the loss of the cationic properties of spruce tannin and its generally lower charge density compared to quebracho tannin. Iron sulfate outperformed both tannin coagulants in

vanadium removal, achieving removal rates of 86% at pH 4, 98% at pH 7, and 100% at pH 9, using lower coagulant doses. However, while iron sulfate requires smaller dosages, it also demands precise control of pH and dosage, which can be challenging in water streams with fluctuating quality. For instance, in vanadium mining processes that involve water recycling, it may be necessary to neutralize the pH of iron sulfate-treated effluents before reuse, leading to increased chemical costs.

X-ray photoelectron spectroscopy analysis of the residues from the coagulation experiments revealed that some of the removed vanadium existed in the less toxic V(IV) oxidation state. Additionally, a photometric dispersion analyzer (PDA 3000, Rank Brothers, UK) equipped with a 5 mm transparent latex tube was used to study floc size, breakage, and regrowth. The quebracho tannin coagulant produced the largest flocs and showed the highest floc regrowth at pH 4 and 7. However, tannin coagulants exhibited no floc regrowth under alkaline conditions, indicating the need for careful flocculation and separation processes. The study also assessed the coagulants' effectiveness in removing dissolved natural organic matter, providing further insights into their performance across different water treatment scenarios.

The potential of acacia as a tannin-based coagulant for removing vanadium from a mine-impacted water

A separate study was conducted using a Mannich-modified acacia tannin coagulant to treat vanadium-contaminated water. The acacia tannin, supplied commercially by Serveyco in Spain, was modified and evaluated for its effectiveness. Charge density analysis of the acacia tannin coagulant revealed a moderate charge density of 4.1 ± 0.28 meq/g at a pH of 4.7 ± 0.22. The vanadium-contaminated effluent used in this experiment was sourced from the Mustavaara mine with an initial vanadium concentration of 44 mg/L. Additionally, the effluent exhibited a turbidity of 5.8 NTU, total surface charge (TSC) of 891 µeq/L, and ultraviolet absorbance at 254 nm (UV_{254}) of 3.8 1/cm. Figure 14 illustrates the performance of the acacia tannin coagulant in treating the vanadium-rich mine water, showing improvements in all measured parameters with increasing coagulant dosage. However, it is important to note that a relatively higher dosage of the acacia tannin coagulant was necessary to achieve a significant reduction in the residual vanadium concentration compared to the quebracho tannin coagulant used in the previous study for neutral pH effluent (Bello et al., 2023).
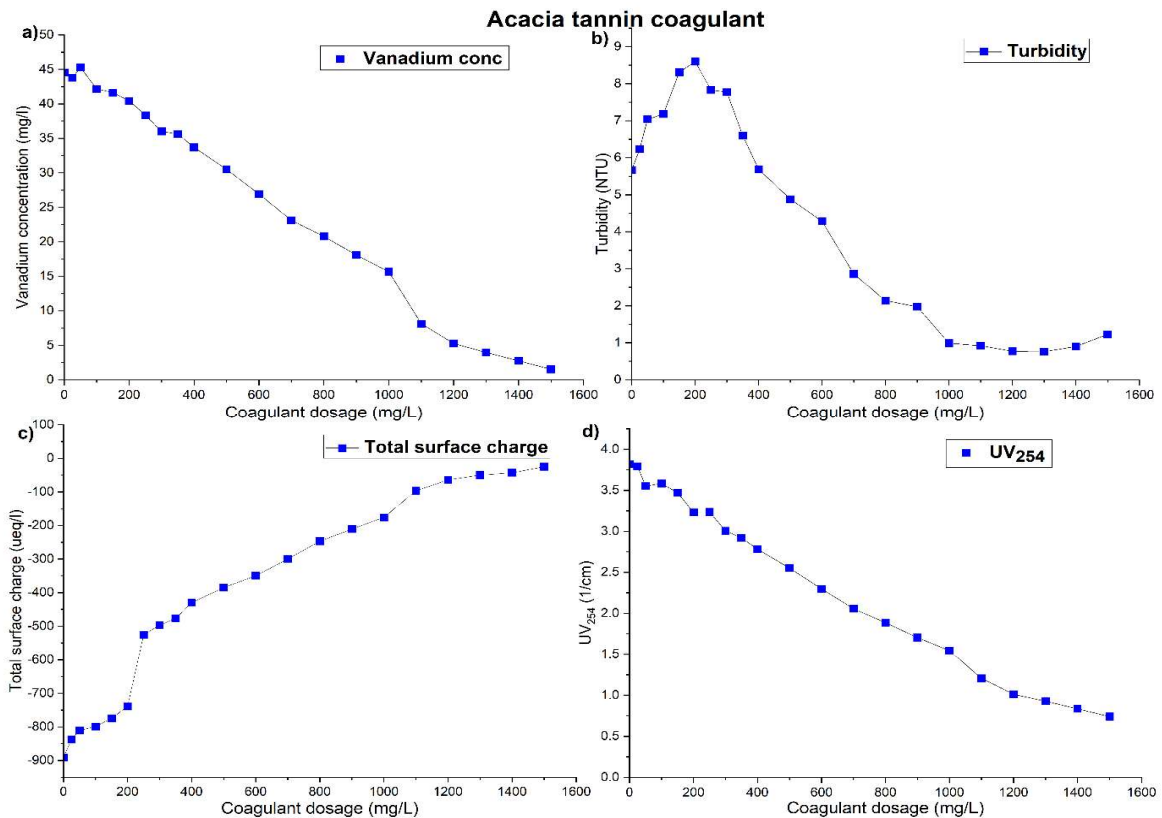
Figure 14. Effect of acacia tannin coagulant dose on a) vanadium removal b) turbidity c) TSC and d) UV$_{254}$ absorbance

WP4 Microbiome analyses

T4.1 Baseline studies and protocols (UCPH)

The goal of this task was to develop standardized protocols for microbiome analyses for each microbial indicator to be used for assessments of water treatment technologies. To do so, two projects were conducted to establish baseline data and protocols for microbiome analyses. These projects include:

Project 1: Changes in density and diversity of *Aeromonas spp.* across sewage treatment plants and water environments and their potential as indicator organisms for the environmental dimension of antibiotic resistance.

In this study, UCPH investigated *Aeromonas* spp. as potential indicator organisms for microbiological analyses. To do this, UCPH enumerated *Aeromonas* spp. from raw sewage and effluents of several wastewater treatment plants (WWTPs) in Denmark, as well as from upstream and downstream locations of the receiving water bodies. Two different selective media (ADA and ASBA) were tested to find the most suitable medium. The taxonomic diversity of the retrieved *Aeromonas* spp. was determined by full-length Sanger sequencing of the 16S rRNA gene, and antibiotic resistance phenotypes were measured through antibiotic susceptibility testing. In addition, diversity was assessed through 16S rRNA gene amplicon sequencing of the full bacterial community to infer cultivation bias. The two different selective media tested had no significant screening preference for species diversity of recovered Aeromonads. However, more phylogenetically diverse isolates could be collected by ASBA. Preliminary analysis at one of the sites (Hillerød, DK) revealed that the diversity of

26

the retrieved *Aeromonas* covered 13 species, with *A. media* dominating in all samples. *A. veronii* and *A. rivipollensis* were abundant in raw and treated wastewaters and in recipient water bodies, respectively. *A. dhakensis* and *A. fluvialis* were only detected in raw wastewater. Wastewater treatment removed > 98% of Aeromonads and tended to reduce the prevalence of antibiotic resistant *Aeromonas* strains. However, we also demonstrated that one specific tetracycline- and piperacillin/tazobactam-resistant *Aeromonas* strain was selectively enriched during wastewater treatment processes and that this strain, or other strains with similar ecological attributes, may be used as indicators of AMR pollution from treated wastewater discharge. These results suggested that WWTP discharges may enhance the dissemination of antibiotic-resistant *Aeromonas*, and some *Aeromonas* spp. strains may be selectively enriched during treatment and subsequently discharged into surface water. This study in addition used high-throughput qPCR of 96 antibiotic resistance genes (ARGs) in order to compare phenotypic and genotypic information on the *Aeromonas* present in the wastewater and stream water samples. Overall, we observed low agreement between resistance patterns in the *Aeromonas* isolates and those inferred from community-level DNA, highlighting the importance of including polyphasic approaches when monitoring AMR in relation to water treatment processes.

This work (Project 1) has been done in collaboration with the Smets/Dechesne group at the Technical University of Denmark and thus represents a collaboration between REWA and the "sister project" BIOCIDE. A paper based on the project was recently published in the Journal of Applied Microbiology (Xu et al., 2025).

Project 2: Removal of viable bacteria and antibiotic resistance genes from wastewater by biochar catalyzed peroxydisulfate oxidation.

The aim of this study was to establish and evaluate a set of methods that can be used to assess the impact of wastewater treatment on the removal of AMR and water quality using microbiome-directed approaches. This work was initiated before REWA partners had developed any new methods, and UCPH thus took advantage of a water treatment technology recently developed by PhD student Chen Wang at the Section for Environmental Chemistry and Physics at UCPH. This water treatment used cyanobacterial biochar produced by pyrolysis at 950°C with phosphorus amendment and acid washing (PCB950w) to activate peroxydisulfate (PDS) to remove AMR from wastewater treatment plant effluent. Selection for AMR among surviving bacteria following treatment and subsequent regrowth potential were investigated in microcosm experiments. The regrowth potential of surviving bacteria was evaluated by bacterial cultivation (CFU) and *in situ* bacterial productivity measurement ([^{3}H] leucine incorporation). The water treatment was able to reduce viable counts of bacteria by >95% and >99.2% within 5 min and 24 hours, respectively. The subsequent regrowth potential of the surviving bacteria following treatment was found to be low, when tested in simulated freshwater- or marine recipients containing intact microbial communities dominated by bacteria that had not been damaged by the imposed harsh water treatment. Based on cultivation-independent techniques (i.e. HT-qPCR of ARGs and 16S rRNA gene amplicon sequencing), the treated bacterial communities contained low levels of antibiotic resistance genes (ARGs) and consisted mainly of members of the *Bacillus* genus, suggesting that mainly spore-forming bacteria survived the water treatment. Only very few strains survived and regrew after treatment, suggesting that biochar-catalyzed PDS treatment can efficiently reduce ARG levels in wastewater. However, the few surviving strains (n=4) grown on *Aeromonas*-specific agar medium, all showed elevated resistance to a number of antibiotics. To further investigate the four surviving isolates, they were whole-genome sequenced together with 13 strains from stream water and WWTP effluent. Surprisingly, taxonomic analysis revealed that the four isolates did not belong to the genus *Aeromonas,* despite being isolated on *Aermonas* specific medium. The isolates

were instead identified as *Paenibacillus pasadensis, Empedobacter falsenii,* and *Pseudomonas aeruginosa*. In contrast, isolates from stream water and WWTP effluent were all classified as *Aeromonas spp*. The genotypic resistance patterns of the four isolates were investigated using CARD, revealing that the *Paenibacillus pasadensis* strains contained ARGs, including vancomycin resistance genes (vanT, vanY, vanW) and phosphonic acid resistance gene (FosBx1). However, these ARGs did not explain the full phenotypic resistance profile of the strains. Similarly, the *Empedobacter falsenii* and *Pseudomonas aeruginosa* strains contained ARGs for resistance to various antibiotics, but these did not match their phenotypic resistance. Hence, further research is needed to explore alternative resistance mechanisms such as stress-induced mutations, regulatory changes, or novel ARGs in these isolates. In conclusion, this study demonstrates that the used combination of methods i.e. regrowth experiments, HT-qPCR gene chip, isolation of *Aeromonas*, and subsequent antibiotic susceptibility testing, is very promising for assessing water treatment systems on AMR and bacteria.

A scientific paper based on the project is in its final stages of preparation and will be submitted for publication in 2025.

T4.2 Co-selection of antibiotic resistance (UCPH)

The goal of this task initially was to assess the impact of novel water treatment processes on antibiotic resistance co-selection potentials in zinc-rich industrial effluents. However, due to changes in the source material in case study #4, the goal was altered to explore the less studied element vanadium, which has not previously been shown to co-select antibiotic resistance.

To investigate vanadium's biotoxicity and its potential to exert selective pressure on microbial communities, we conducted a bioluminescence assay using the genetically modified *Nitrosomonas europaea* bioreporter strain. The bioreporter was exposed to increasing concentrations of sodium metavanadate (NaVO₃). The results revealed that sodium metavanadate inhibited the bioreporter strain in a dose-dependent manner, with a half-maximal effective concentration (EC50) of approximately 2682 mg/L of vanadium (Figure 15). Although vanadium demonstrated the ability to exert selective pressure on the bioreporter strain, a relatively high concentration was required to induce significant inhibition—far exceeding the concentrations typically found in environmental settings ((Zhang et al., 2023). This finding aligns with another study, which reported an EC50 of 54.9 mM (6691.86 mg/L) for a *Pseudomonas putida* bioreporter strain, while no inhibitory effects were observed on *Escherichia coli* and *Vibrio fischeri* bioreporter strains even at concentrations up to 100 mM (Bell et al., 2004).
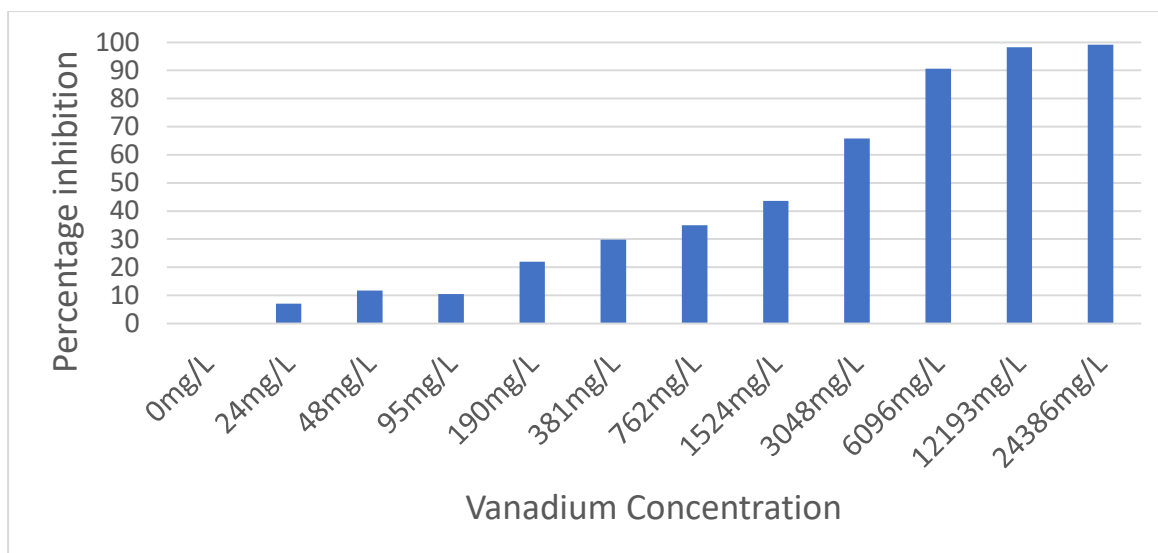
Figure 15. Inhibition (%) of bioreporter strain *Nitrosomonas europaea* by water samples collected at the Mustavaara vanadium mining site in Finland. Reference water (Reference stream) was collected from a stream running through the site and water samples with high vanadium content (Mine Ditch), were collected from two ditches located at the site

To further investigate the potential for co-selection of vanadium and antibiotic resistance, we explored the phenotypic co-occurrence of vanadium and antibiotic resistance in a collection of *Aeromonas spp*. isolates derived from vanadium-contaminated sediment and a reference sediment sample collected at the same Finnish site. Results showed that all isolates exhibited a limited level of vanadium and antibiotic resistance, with no difference between isolate origin (vanadium contaminated vs. reference sediment). In conclusion, our results indicate a negligible risk for co-selection of antibiotic resistance in vanadium-contaminated waters.

T4.3 Final assessment of case studies (UCPH)

Case study #1, surface water treatment (MIGAL)

We investigated the use of clay-based coagulants to improve the pretreatment of cattle farm wastewater by reducing pathogen risks. The primary aim was to evaluate whether treating cowshed wastewater with clay-based coagulants could effectively reduce the abundance of virulence factor genes (VFGs), thereby lowering the risk of pathogen transmission when effluents or sludge are used as fertilizer or discharged into local wastewater treatment plants.

To achieve this, experiments were conducted using three coagulants: sepiolite-polydadmac (NC), kaolinite-polydadmac (DKG), and the conventional coagulant alum. DNA was extracted from treated wastewater samples, and the abundances of VFGs and total bacteria were determined using an HT-qPCR chip recently developed by collaborators in China (Xie et al., 2023). Changes in microbial community composition were assessed by 16S rRNA gene amplicon sequencing, while chemical wastewater quality (toxicity) was using a recently developed high-throughput bioluminescence inhibition assay based on a genetically modified *Nitrosomonas europaea* bioreporter strain.

The project has experienced delays due to the situation in northern Israel and parental leaves, but data analysis and manuscript preparation are ongoing and are expected to be completed in the spring of 2025.

Case study #2, sewage effluent treatment (UO)

The impact of the biosorbent column treatment on viable bacteria and biotoxicity in the tested wastewater from the pilot study was evaluated using Colony Forming Unit (CFU) counting and biotoxicity measurements with the whole-cell bioreporter strain *Nitrosomonas europaea*, respectively. Before regeneration of the column material, the CFU levels were higher in untreated wastewater samples (avg. 50,000 CFU/mL) compared to those treated by the biosorbent (avg. 22,833 CFU/mL). This suggests that the fresh biosorbent materials effectively reduce bacterial counts in the wastewater.

However, after regeneration of the biosorbent, the CFU levels surged dramatically in the treated samples, reaching 950,000 CFU/mL, compared to 100,500 CFU/mL in the untreated wastewater. This indicates that the 0.2 M NaOH used for regeneration causes the biosorbent to release previously adsorbed contaminants, including bacteria that adhered to the material.

Biotoxicity was assessed using a bioluminescence assay with *N. europaea* to evaluate wastewater toxicity to a relevant, sensitive test organism. No significant toxicity was observed in either the untreated wastewater or the biosorbent-treated samples, except for a transient effect immediately after biosorbent column regeneration. Hence, the highest biotoxicity (73.7% inhibition) occurred post-regeneration, likely due to contaminants released from the biosorbent, but it stabilized at low background levels after 10 days. The results were recently published in Environmental Research (Mohammadzadeh et al., 2025).

Case study #3, sewage effluent treatment (UKZN)

The impact of red phosphorus/bismuth oxybromide/g-C3N4 (BiBrP) and tin vanadate/g-C3N4/WO3/Bi2WO6 on bacterial activity and viability was assessed in a bench-scale experiment. The experiment involved mixing the photocatalytic materials with 20 mL of wastewater effluent from the Avedøre Rensningsanlæg municipal wastewater treatment plant (Denmark) in 100 mL beakers, stirred using a magnetite stirrer under visible light (40 W light bulb). Two different concentrations (500 and 1500 mg/L) of each material were tested, with samples collected at intervals of 10 minutes, 2 hours, 4 hours, 6 hours, and 8 hours of contact time. The bacterial growth rate was determined using the [3H]leucine incorporation technique (pmol Leucine/h/mL), while bacterial viability (CFU/mL) was quantified by cultivation on Reasoner's 2A agar (R2A) and Ampicillin-Dextrin-Agar to assess heterotrophic bacteria and *Aeromonas* spp., respectively. The experiment included three biological replicates, with controls conducted both with and without the light source.

At the highest concentration of BiBrP, some inhibition of [3H]leucine incorporation was observed after 120 minutes compared to the controls, indicating an inhibitory effect of the treatment on bacterial productivity (growth). However, bacterial viability (CFU/mL) was not significantly affected, demonstrating that bacterial growth inhibition could not be linked to reduced bacterial survival (Figure 16). For tin vanadate, we did not observe a consistent impact on either bacterial growth or viability, indicating a limited impact of the treatment on wastewater bacteria (Figure 17).
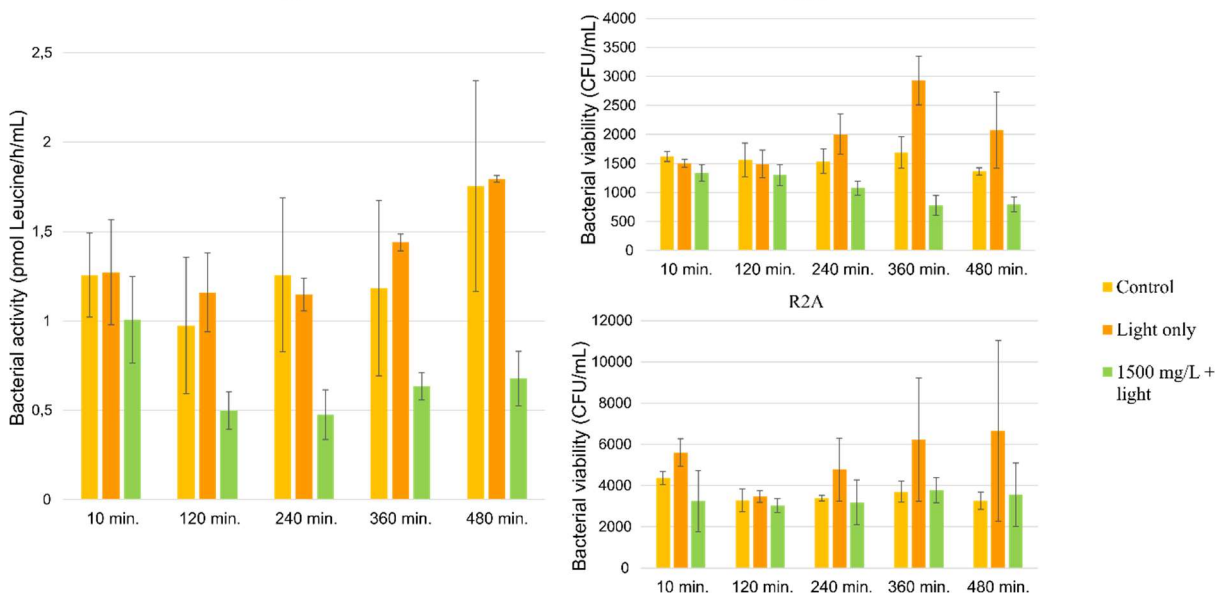
Figure 16. Bacterial growth ([^{3}H]leucine incorporation) and viability (colony-forming units) of *Aeromonas spp.* (ADA) and heterotrophic bacteria (R2A) in waste water following treatment with 1500 mg/L of red phosphorus/bismuth oxybromide/g-C3N4 (BiBrP). Control = Wastewater; Light only = Wastewater emitted with light; 1500 mg/L+light = wastewater mixed with 1500 mg/L of BiBrP and emitted with light
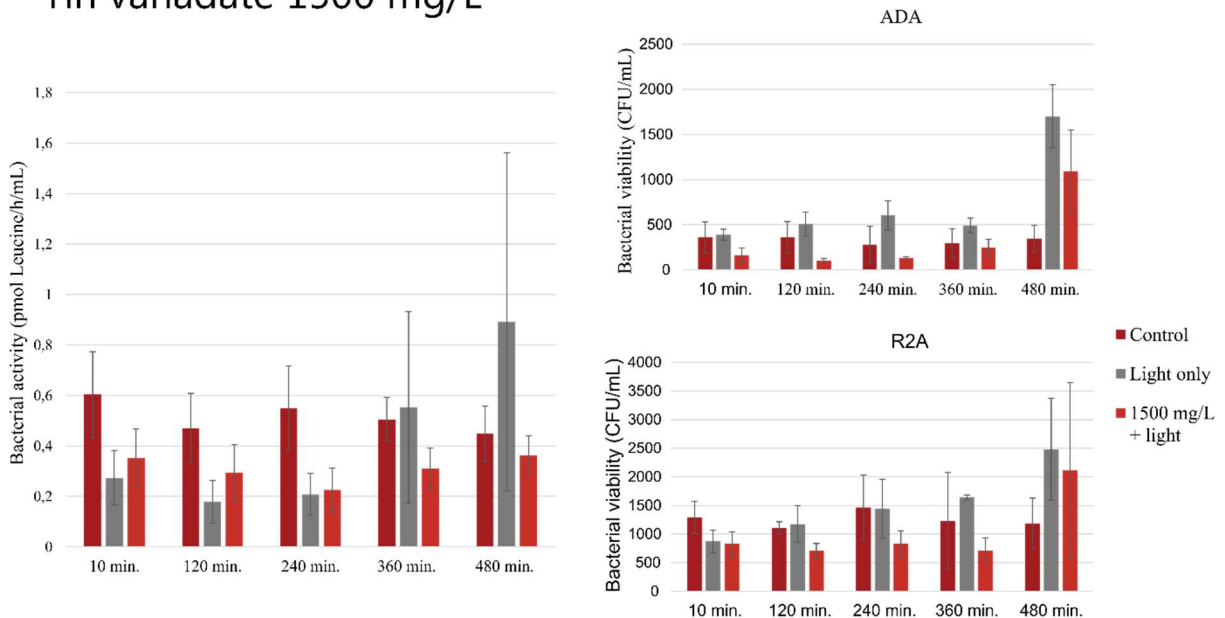
Figure 17. Bacterial growth ([^{3}H]leucine incorporation) and viability (colony-forming units; CFU) of *Aeromonas spp.* (ADA) and heterotrophic bacteria (R2A) in waste water following treatment with 1500 mg/L of tin vanadate/g-C3N4/WO3/Bi2WO6. Control = Wastewater; Light only = Wastewater emitted with light; 1500 mg/L+light = wastewater mixed with 1500 mg/L of Tin vanadate and emitted with light

Case study #4, metal-rich effluent (UO)

To assess whether the removal of vanadium by acacia tannin coagulants affected the biotoxicity of the mining water, researchers measured the response of the *N. europaea* bioreporter strain to treated water samples (Figure 18). Despite the reduction in vanadium levels with increasing doses of the coagulant, there was no significant change in the biotoxicity of the mining water. These findings indicate that vanadium contributed minimally to the observed biotoxicity in the effluent. Collectively, our results (please also see T4.2 above) indicate that elevated vanadium levels from the investigated mining site pose a negligible risk for co-selection of antibiotic resistance. However, the mining water did exhibit some inhibitory effects on the bioreporter strain, suggesting that other chemicals in the mining effluents did adversely affect water quality.
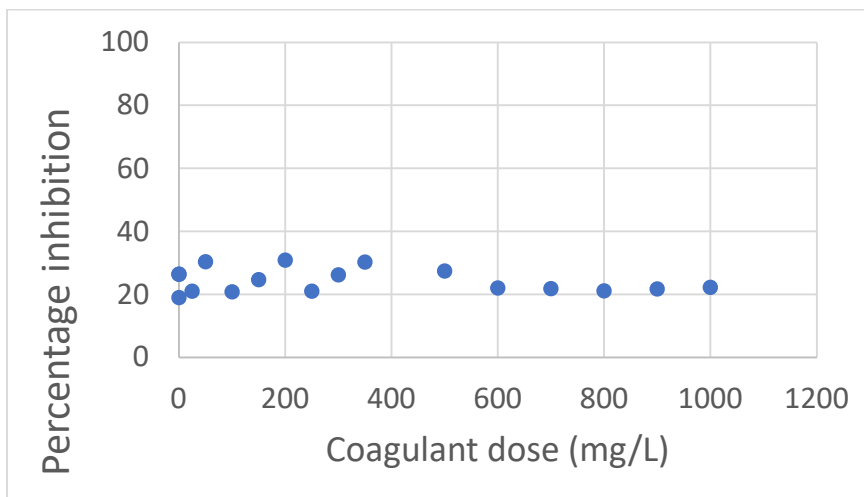
Figure 18. Inhibition (%) of bioreporter strain *Nitrosomonas europaea* by vanadium mining water samples treated with increasing doses of the acacia tannin coagulant to remove vanadium in the water.

Conclusion

The project developed effective methods for removing contaminants of emerging concern (CECs) from polluted waters, with a focus on technologies for water reuse. Key achievements include the synthesis of sustainable materials for pollutant removal and the evaluation of equipment and procedures used in pilot projects, which support future scaling efforts. The project demonstrated the practical effectiveness of water treatment technologies in cleaning polluted surface water, sewage effluents, and metal-rich wastewater. Wood-based biosorbents were highly effective in removing pharmaceuticals and antibiotics. Photocatalysts also showed promise for breaking down antibiotics using visible light, while tannin-based coagulants were particularly effective in removing vanadium from metal-rich effluents.

The project has also delivered a guideline (D4.3) for microbiome-directed testing of bench-scale water treatment technologies. Based on the experiences obtained in the REWA project, the guideline emphasizes a tiered, polyphasic approach and provides guidance on how to assess both the benefits and risks of emerging water treatment technologies already at the bench or pilot scale prior to full-scale implementation.

In summary, the project's approach successfully reduced CEC levels through advanced material synthesis, adsorption, and photocatalytic degradation. Future research should focus on optimizing scalability for large-scale water treatment plants, assessing long-term environmental impacts and cost-effectiveness, and combining these methods with emerging technologies. Testing the systems in various real-world conditions would help evaluate their performance across different types of contaminated water.

References

Bell, J. M. L., Philp, J. C., Kuyukina, M. S., Ivshina, I. B., Dunbar, S. A., Cunningham, C. J., & Anderson, P. (2004). Methods evaluating vanadium tolerance in bacteria isolated from crude oil contaminated land. *Journal of Microbiological Methods*, *58*(1), 87–100. https://doi.org/10.1016/j.mimet.2004.03.006

Bello, A., Martincigh, B. S., Nyamori, V. O., & Leiviskä, T. (2023). Vanadium removal and floc characteristics of tannin biocoagulants and iron sulphate in the treatment of mine effluent. *Chemical Engineering Journal*, *476*, 146665. https://doi.org/10.1016/j.cej.2023.146665

Kumar, T. R., & Umamaheswari, S. (2011). FTIR, FTR and UV-Vis Analysis of Carbamazepine. *Research Journal of Pharmaceutical, Biological and Chemical Sciences*, *2*(4), 685–693.

Madejová, J., & Komadel, P. (2001). Baseline studies of the clay minerals society source clays: Infrared methods. *Clays and Clay Minerals*, *49*(5), 410–432. https://doi.org/10.1346/CCMN.2001.0490508

Mohammadzadeh, M., Bello, A., Lassen, S. B., Brandt, K. K., Risteelä, S., & Leiviskä, T. (2025). Pilot-scale adsorption of pharmaceuticals from municipal wastewater effluent using low-cost magnetite-pine bark: Regeneration/enumeration of viable bacteria with a study on their biotoxicity. *Environmental Research*, *268*. https://doi.org/10.1016/j.envres.2025.120774

Mohammadzadeh, M., & Leiviskä, T. (2023). Iron-modified peat and magnetite-pine bark biosorbents for levofloxacin and trimethoprim removal from synthetic water and various

pharmaceuticals from real wastewater. *Industrial Crops and Products*, *195*. https://doi.org/10.1016/j.indcrop.2023.116491

Rytwo, G., Levy, S., Shahar, Y., Lotan, I., Zelkind, A. L., Klein, T., & Barak, C. (2024). Health protection using clay minerals: A case study based on the removal of BPA and BPS from water. *Clays and Clay Minerals*, *69*(5). https://doi.org/10.1007/s42860-021

Rytwo, G., & Zelkind, A. L. (2022). Evaluation of kinetic pseudo-order in the photocatalytic degradation of ofloxacin. *Catalysts*, *12*(1). https://doi.org/10.3390/catal12010024

Xie, S. T., Ding, L. J., Huang, F. Y., Zhao, Y., An, X. L., Su, J. Q., Sun, G. X., Song, Y. Q., & Zhu, Y. G. (2023). VFG-Chip: A high-throughput qPCR microarray for profiling virulence factor genes from the environment. *Environment International*, *172*. https://doi.org/10.1016/j.envint.2023.107761

Xu, J., Jensen, M. K. S., Lassen, S. B., Brandt, K. K., Dechesne, A., & Smets, B. F. (2025). *Aeromonas* isolation reveals this genus's contribution to antimicrobial resistance fluxes across the wastewater–treated water–river interface. *Journal of Applied Microbiology*, *136*(1). https://doi.org/10.1093/jambio/lxae302

Zhang, B., Zhang, H., He, J., Zhou, S., Dong, H., Rinklebe, J., & Ok, Y. S. (2023). Vanadium in the Environment: Biogeochemistry and Bioremediation. In *Environmental Science and Technology* (Vol. 57, Issue 39, pp. 14770–14786). American Chemical Society. https://doi.org/10.1021/acs.est.3c04508